Italian National Agency for New Technologies, Energy and Sustainable Economic Development

Analysis of Runaways Mitigation in JET with Shattered Pellet Injection

Paolo Buratti
paoloburatti2@gmail.com

WIP 21/06/2022

Shattered Pellet Injection (SPI)

- Pellet criogenico frammentato per aumentare la superficie di interazione col plasma
- Convertire l'energia del plasma in radiazione per alleviare il carico termico nelle disruptions
- Mitigare i fasci di runaway electrons (RE) eventualmente prodotti durante le disruptions
- Diverse dimensioni e diversi dosaggi di D_2, Ne, Ar

Visual: big Ne shattered pellet

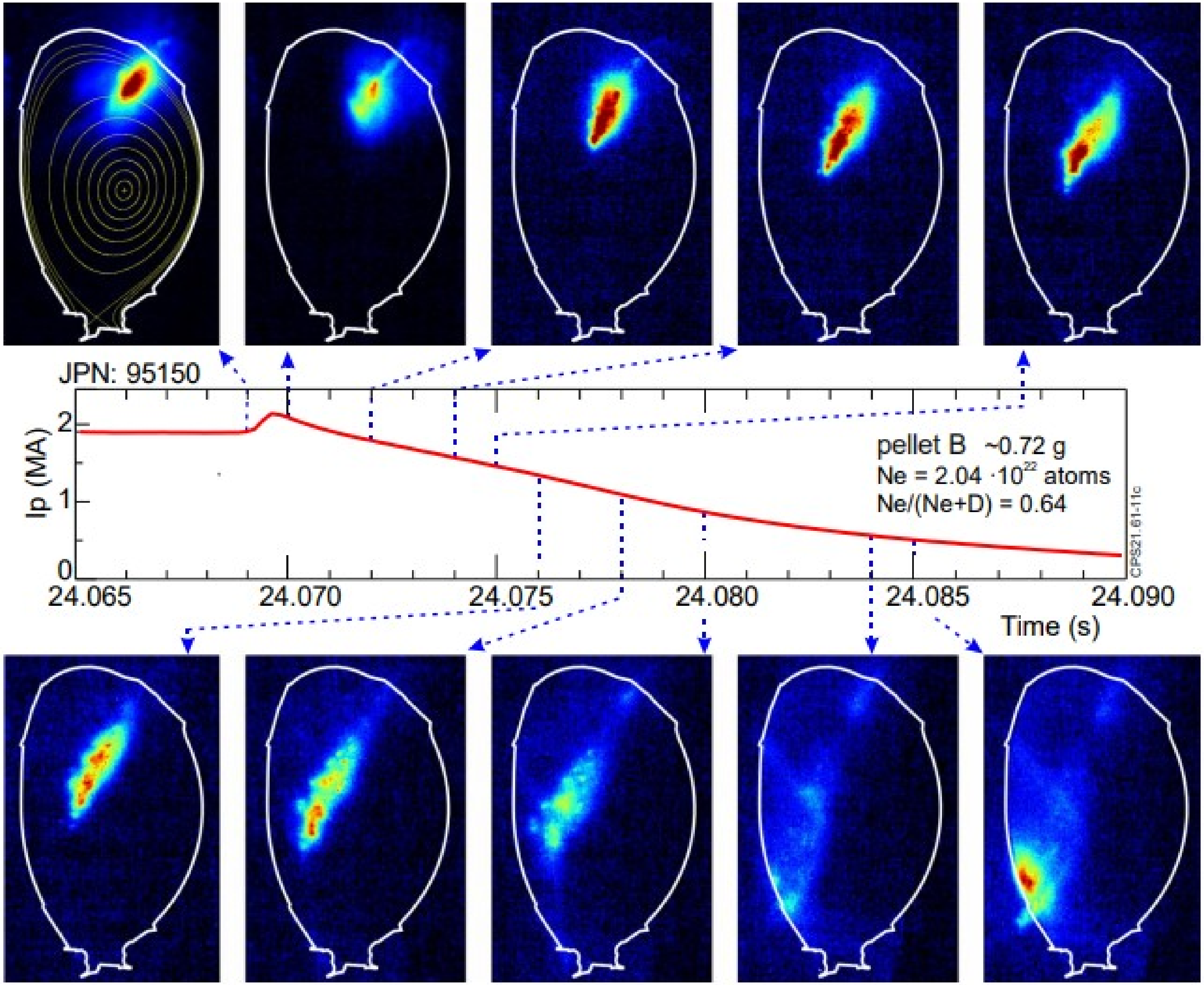

Esperimenti di RE safe termination al JET

PHYSICAL REVIEW LETTERS **126,** 175001 (2021)

Demonstration of Safe Termination of Megaampere Relativistic Electron Beams in Tokamaks

Cédric Reux*

- Disruption (indotta da Ar Massive Gas Injection) che trasferisce parte della corrente di plasma ad un fascio di runaway electrons
- SPI per ottenere la safe termination del fascio
- Safe = senza provocare evidenza riscaldamento della parete sulle termocamere all'infrarosso.

Esperimenti di safe termination al JET (2)

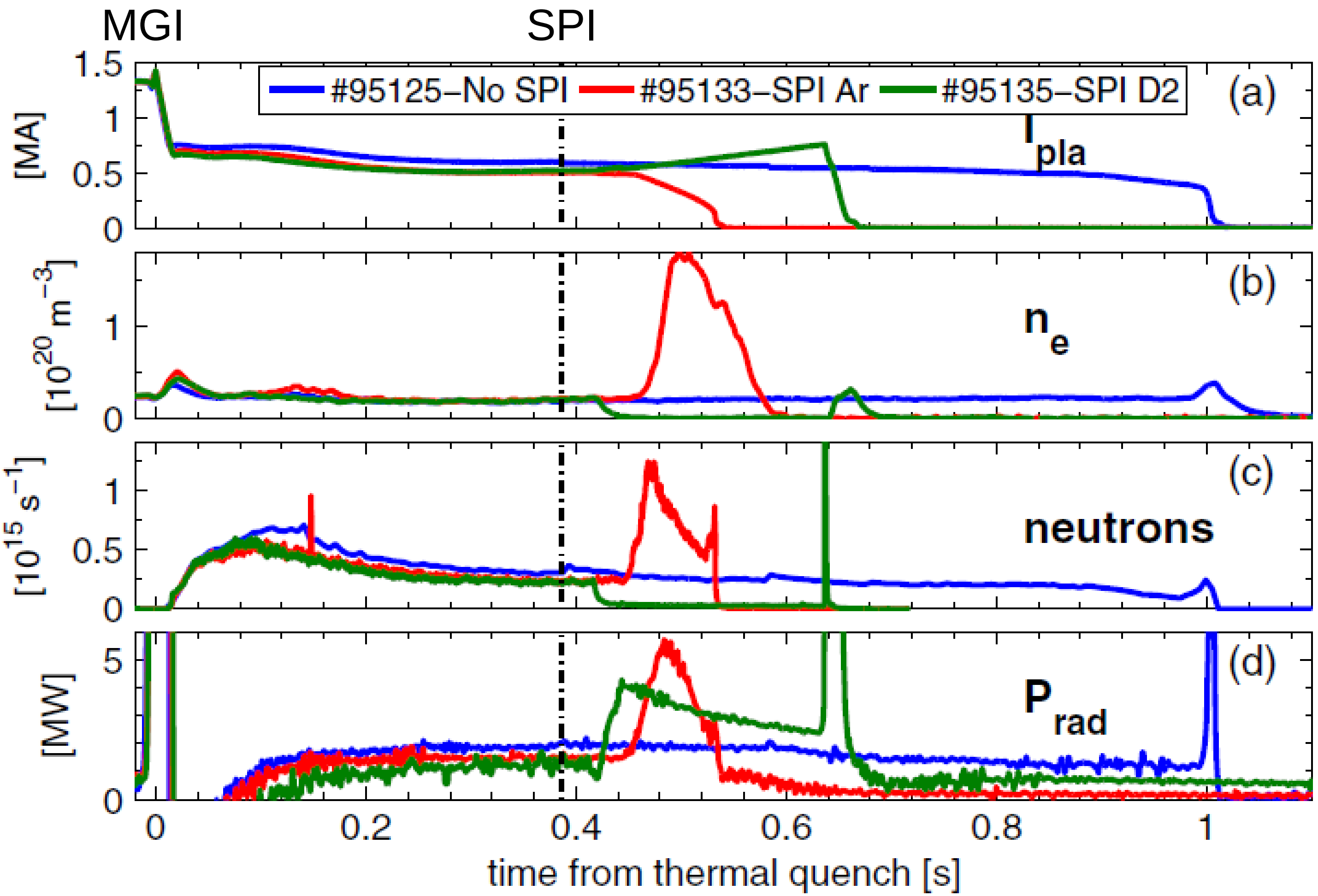

- Safe termination in verde
- Ricomparsa di plasma termico durante il collasso finale

Esperimenti di safe termination al JET (3)

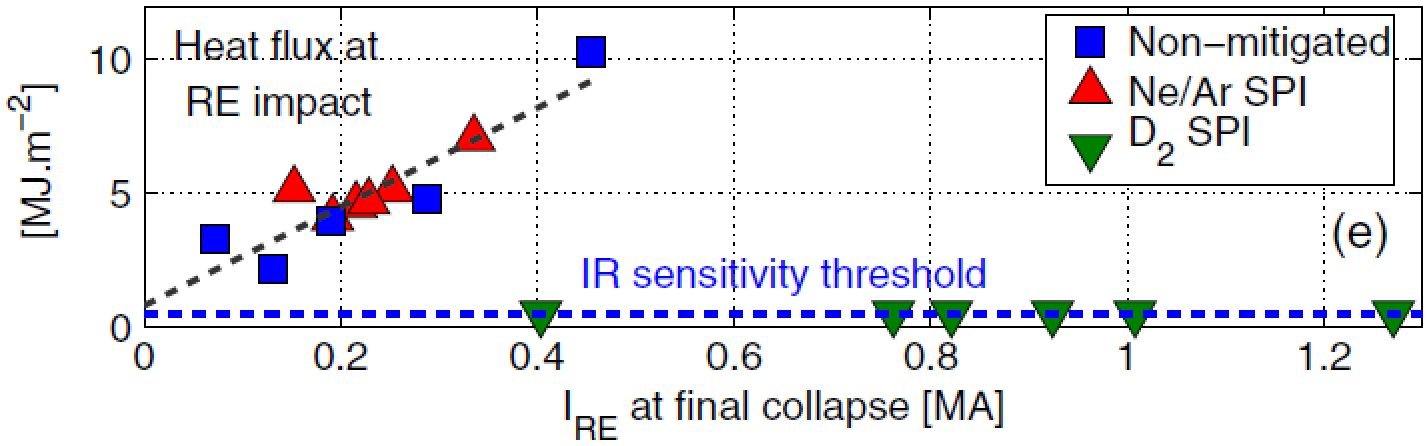

- In assenza di SPI o con SPI ad alto Z il carico sulla parete è importante e aumenta con la corrente
- Safe termination ottenuta con D_2 SPI fino a correnti del fascio runaway > 1MA

Esperimenti di safe termination al JET (4)

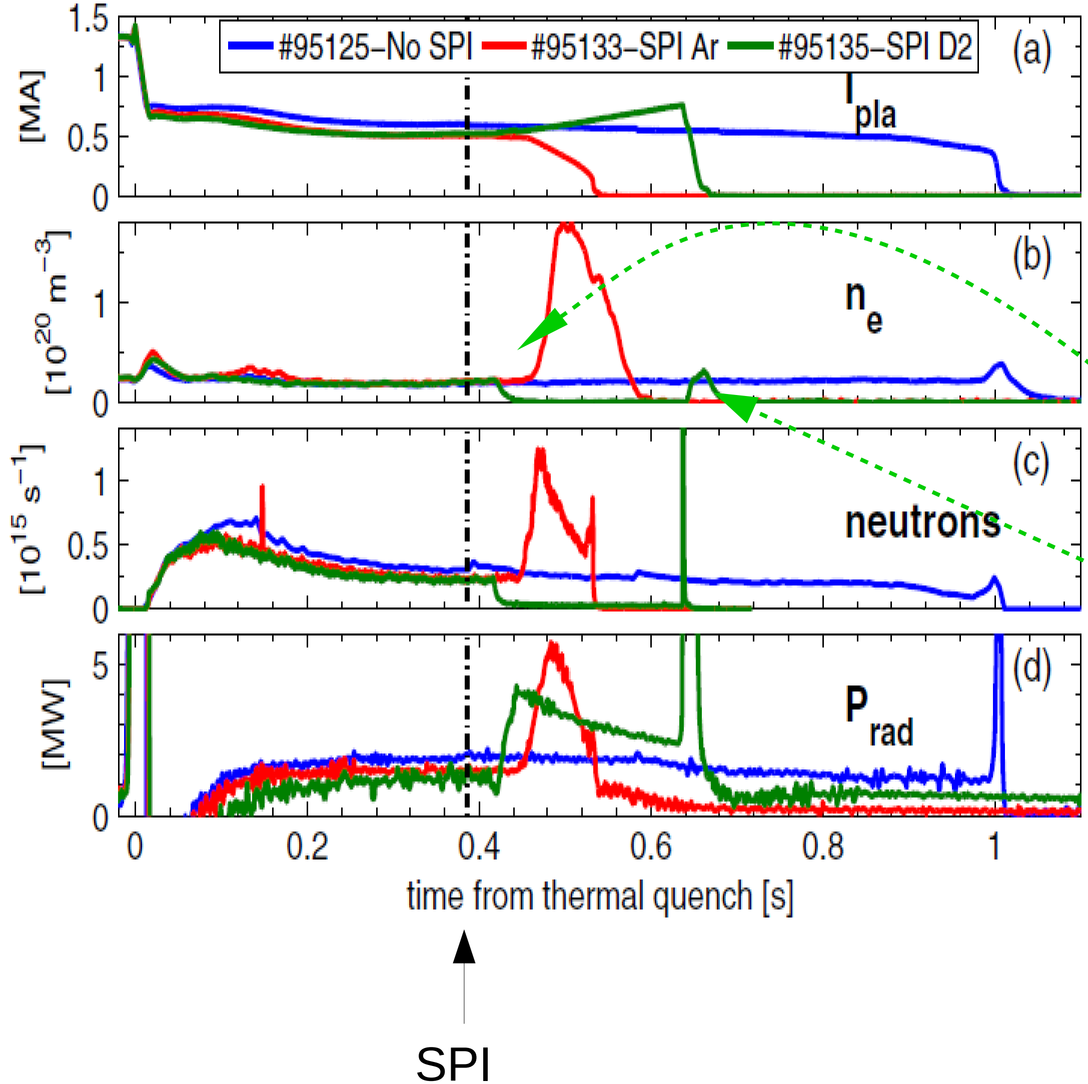

Nel caso D_2 (in verde):

- La corrente aumenta
- Ar lasciato da MGIdiminuisce (purge)
- La densità diminuisce (cooling e ricombinazione)
- La densità ricompare alla fine: l'energia è trasferita a plasma termico.

Analisi di dettaglio

- L' Electron Cyclotron Emission aumenta in risposta all'iniezione di shattered pellets di Deuterio: da spiegare (spiegazione nel seguito)

- Si osservano bursts di attività magnetica da interpretare: instabilità cinetiche tipo anomalous Doppler, o modi MHD? (la seconda)

- Si osservano strutture island-like rotanti nei filmati di emissione di sincrotrone: ricerca di correlazioni con la magnetica (lavoro non competato).

Analysis of ECE response to SPI

P. Buratti

M18-36 meeting 17 June 2021

ITALIAN NATIONAL AGENCY FOR NEW TECHNOLOGIES, ENERGY AND SUSTAINABLE ECONOMIC DEVELOPMENT

This work has been carried out within the framework of the EUROfusion Consortium and has received funding from the European Union's Horizon 2020 research and innovation programme under grant agreement number 633053. The views and opinions expressed herein do not necessarily reflect those of the European Commission.

Outline

- ECE spectra variations in response to MGI and SPI
- A toy model for ECE spectra and its results
- Fast transients and their interpretation

ECE response to MGI and SPI

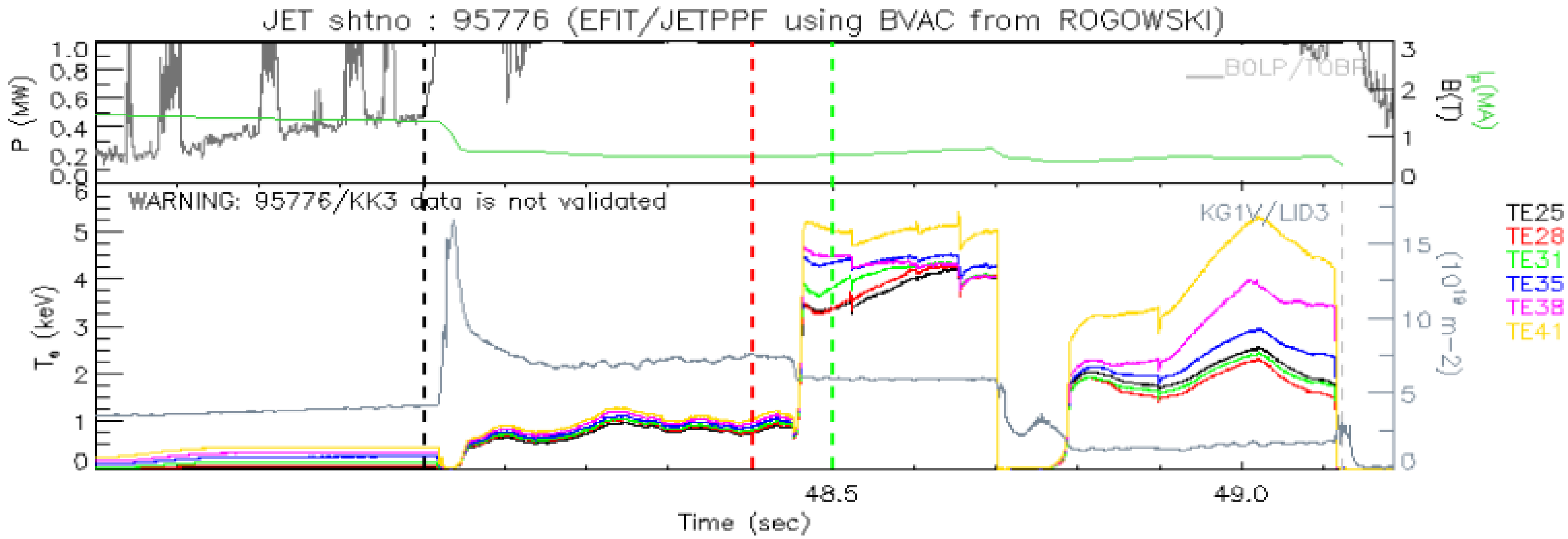

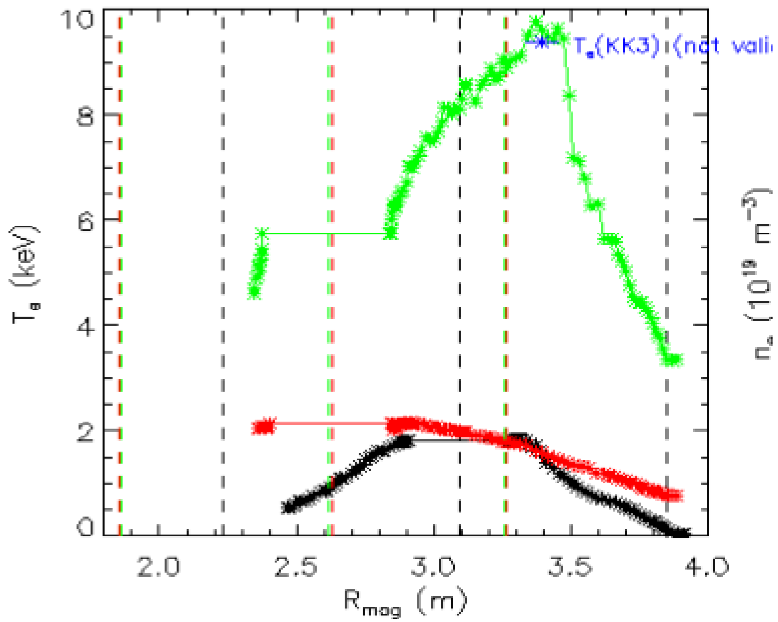

t = 8.0 thermal plasma

t = 8.4 post-MGI
need extended spectral
analysis (ECM1) to clarify

t = 8.5 post-SPI
very different shape

ECM1 T_{rad} analysis

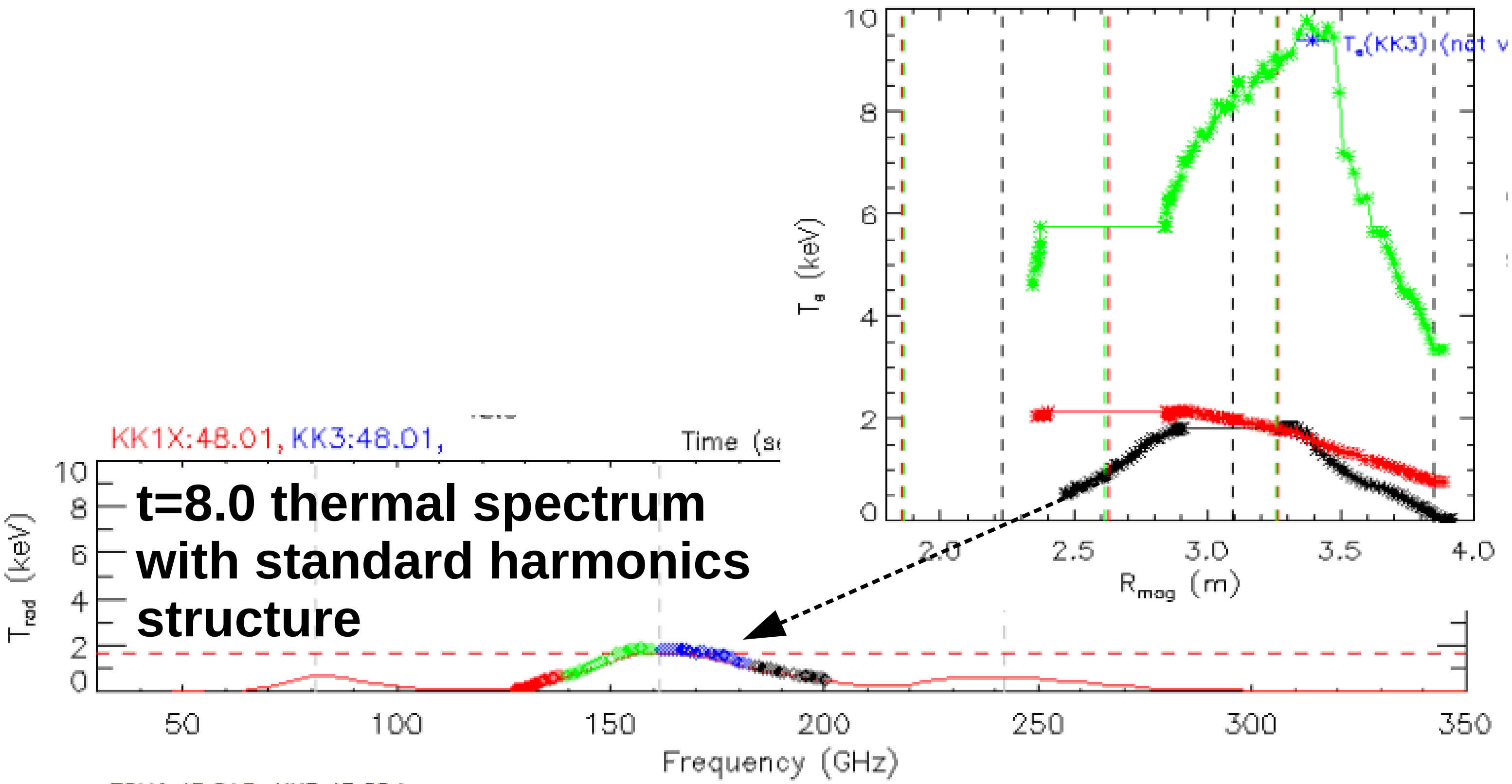

t=8.0 thermal spectrum with standard harmonics structure

ECM1 T_{rad} analysis

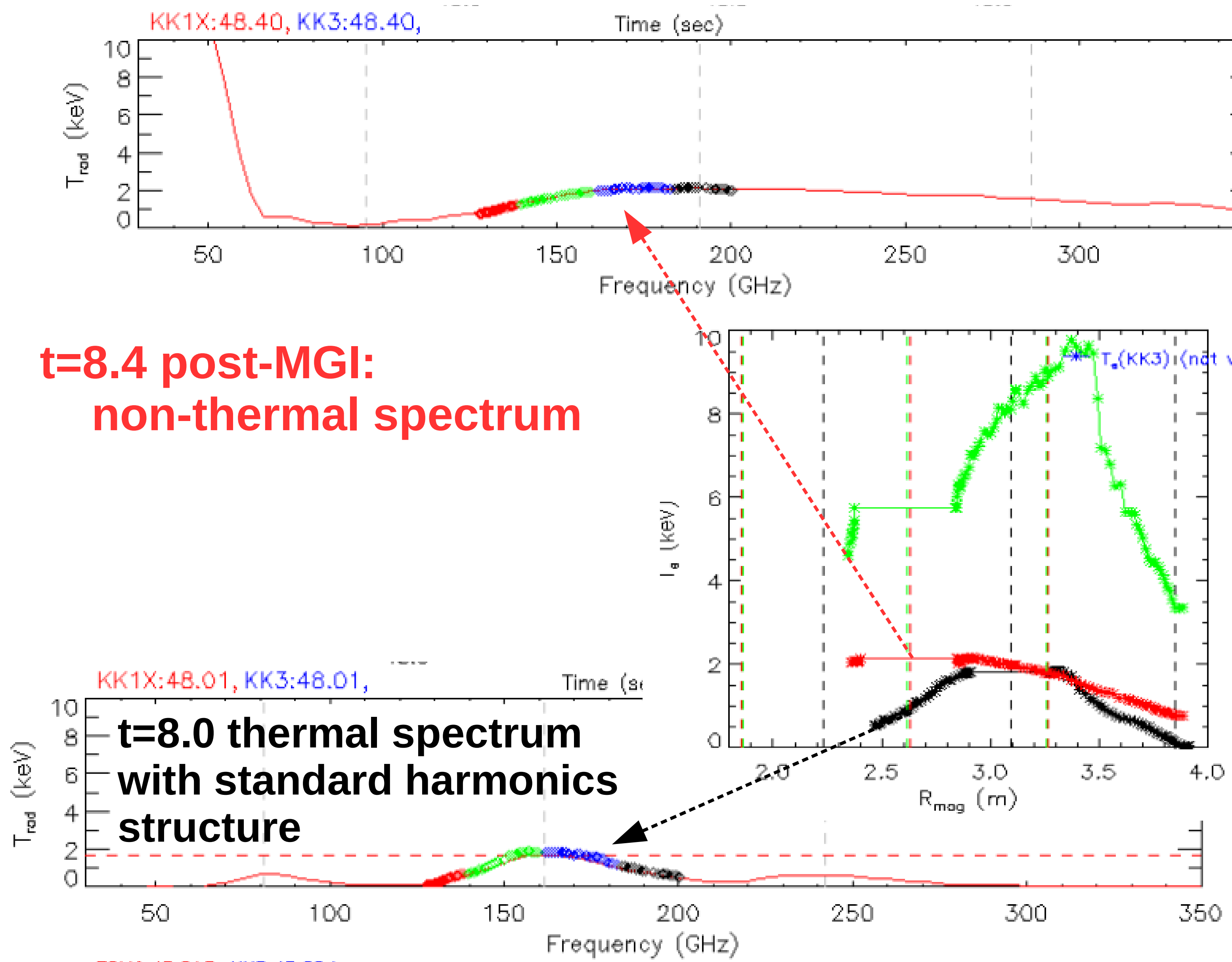

ECM1 T_{rad} analysis

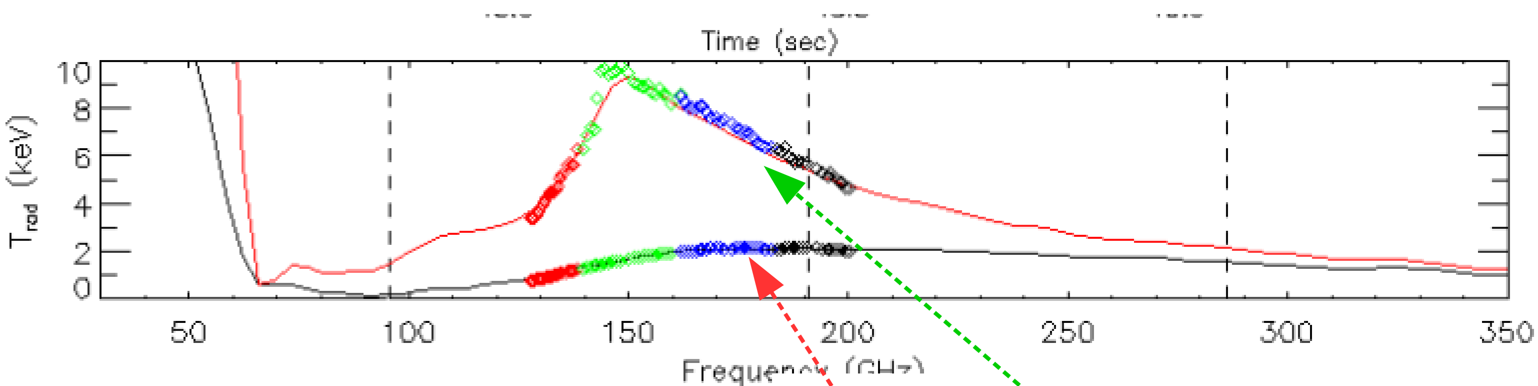

t=8.4 post-MGI:
non-thermal spectrum

t=8.5 post-SPI
more intense and more
structured non-thermal

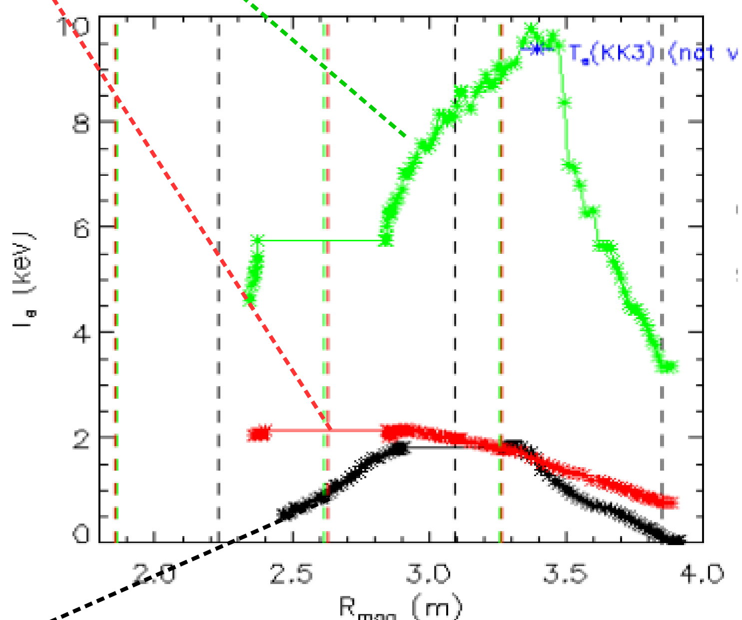

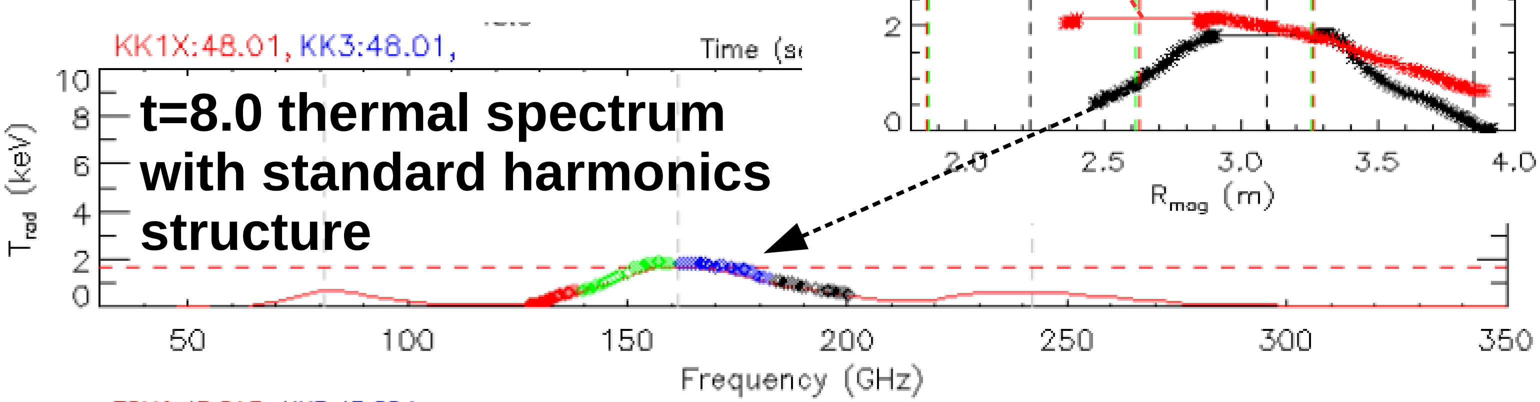

t=8.0 thermal spectrum
with standard harmonics
structure

ECM1 intensity analysis

- Use full 30-500 GHz spectra from KK1 interferometer
- Intensity is power per unit frequency, solid angle, area

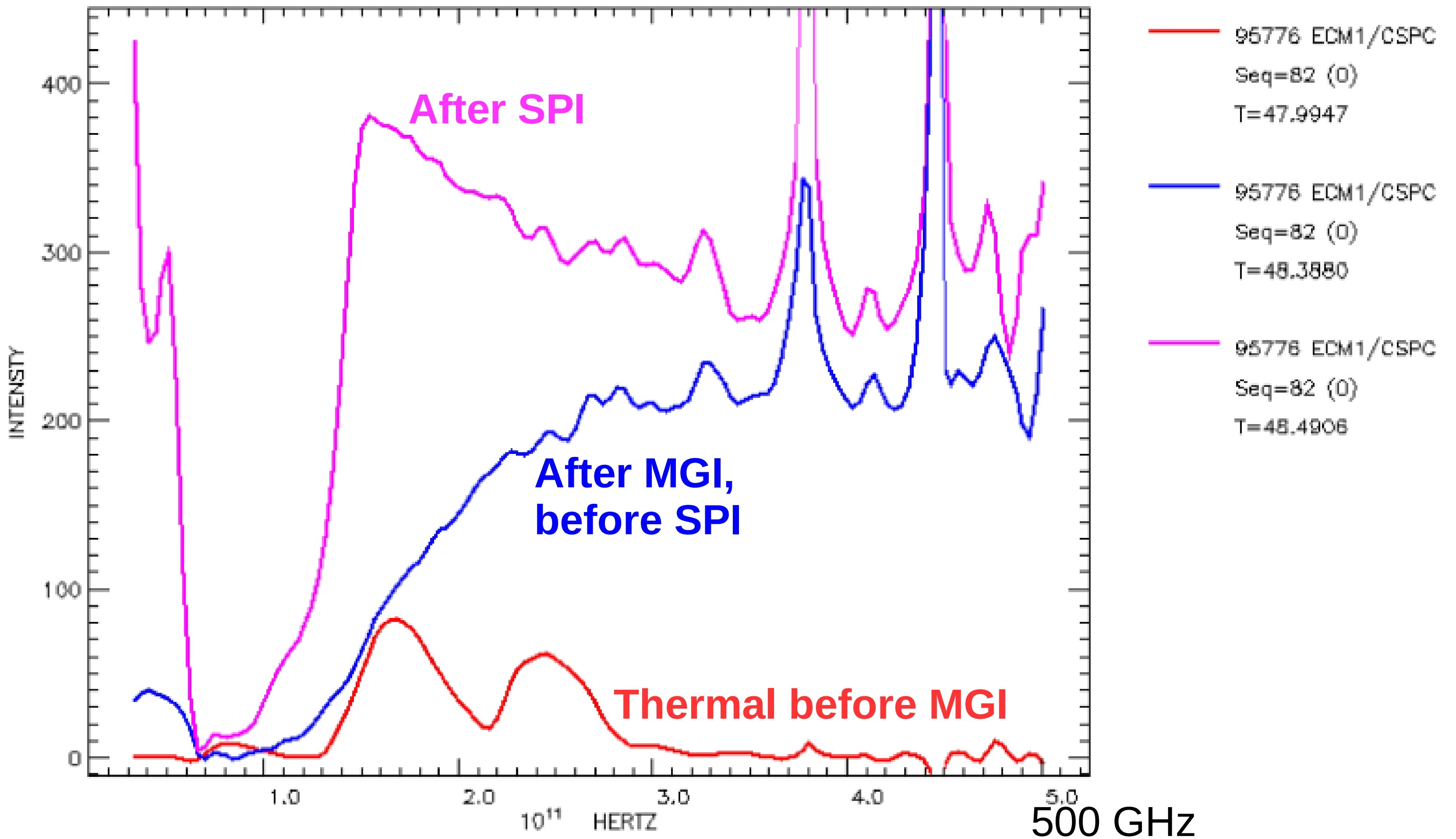

ECM1 intensity analysis

Calibration problems at 380 and 448 GHz (due to H_2O_{vap} in air), good data in between

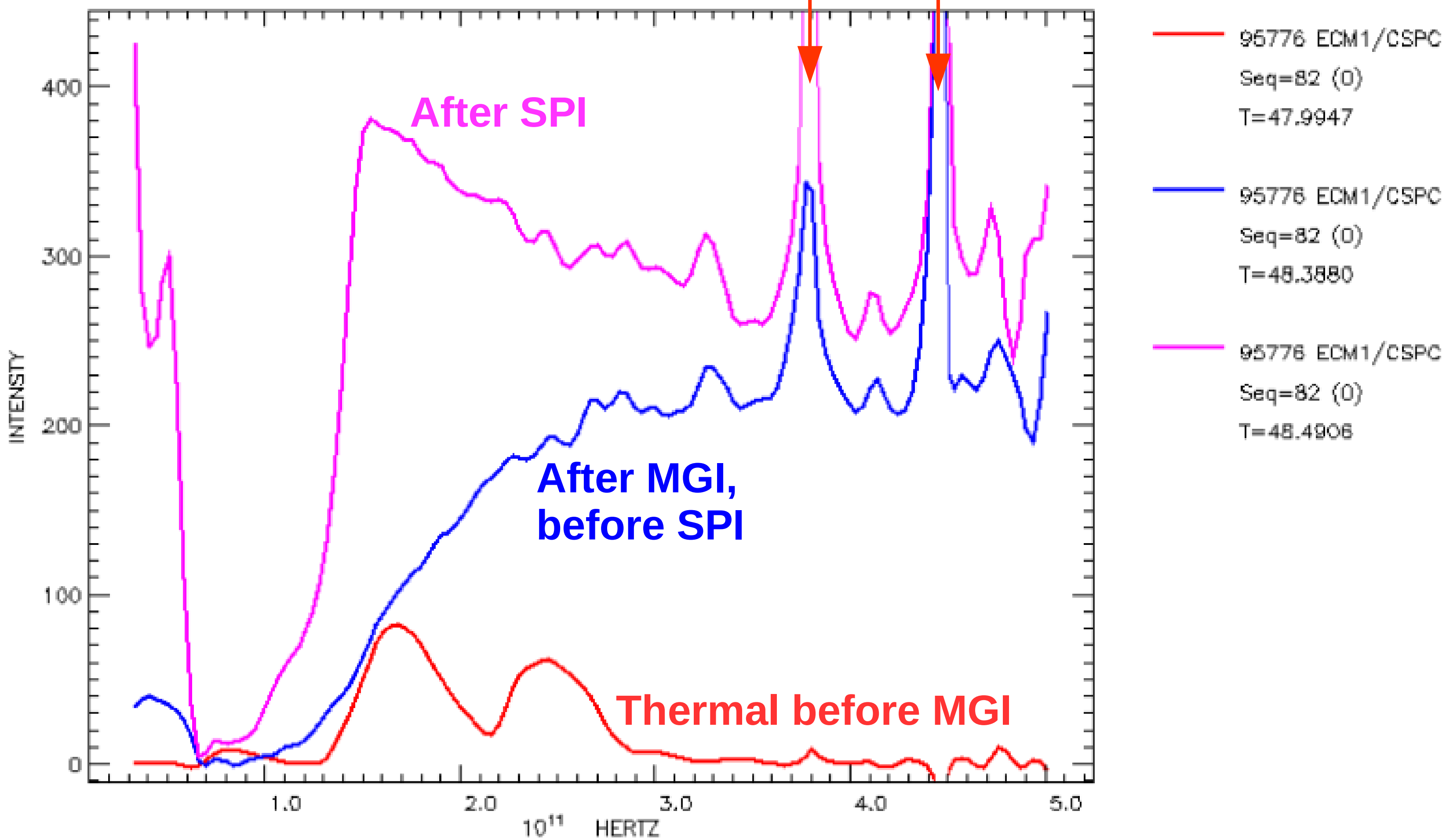

ECM1 intensity analysis

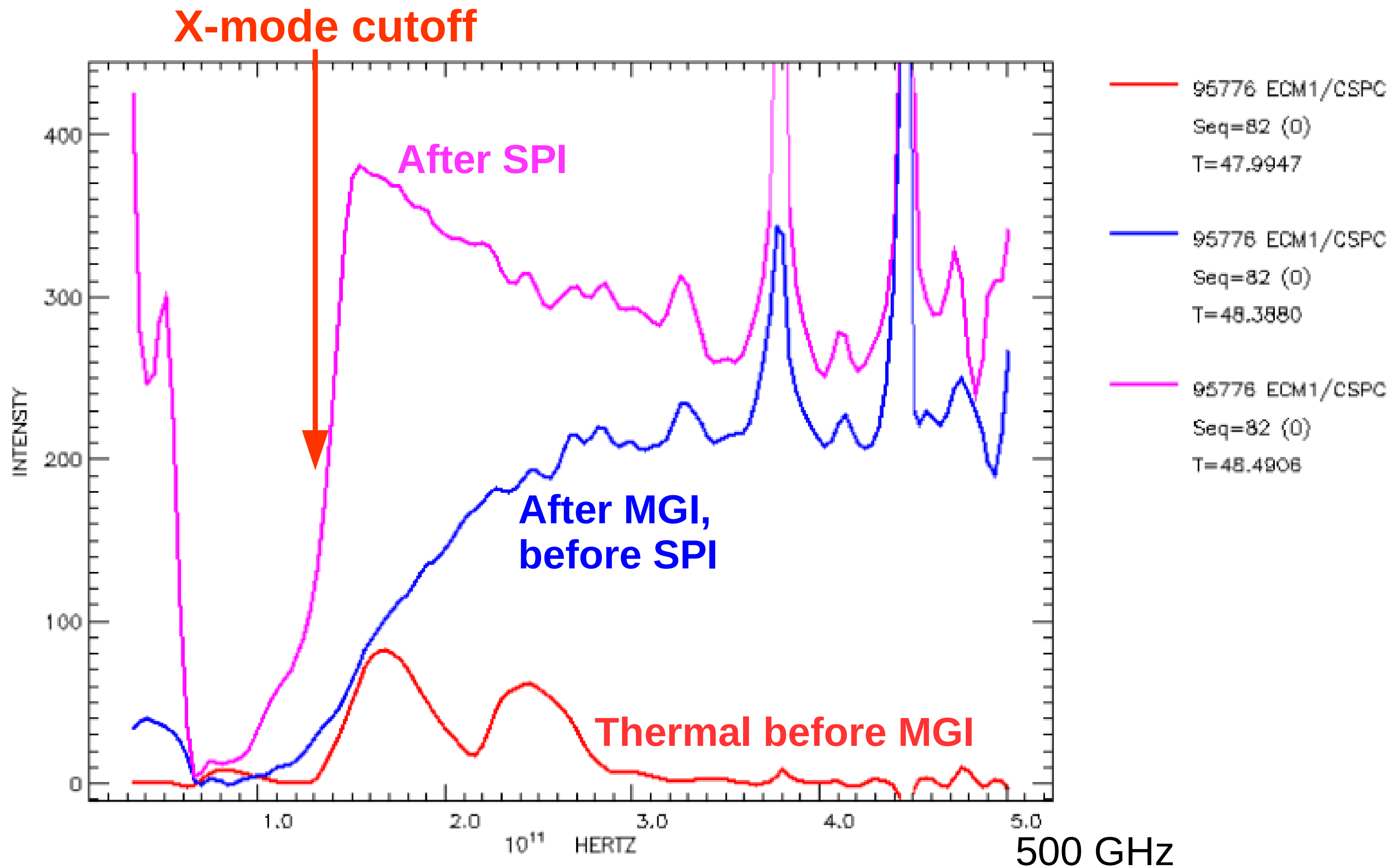

Evolution of ECE spectra

Follow time evolution:

at 146 GHZ, where variation is larger, and

410 GHz, where thermal emission is negligible

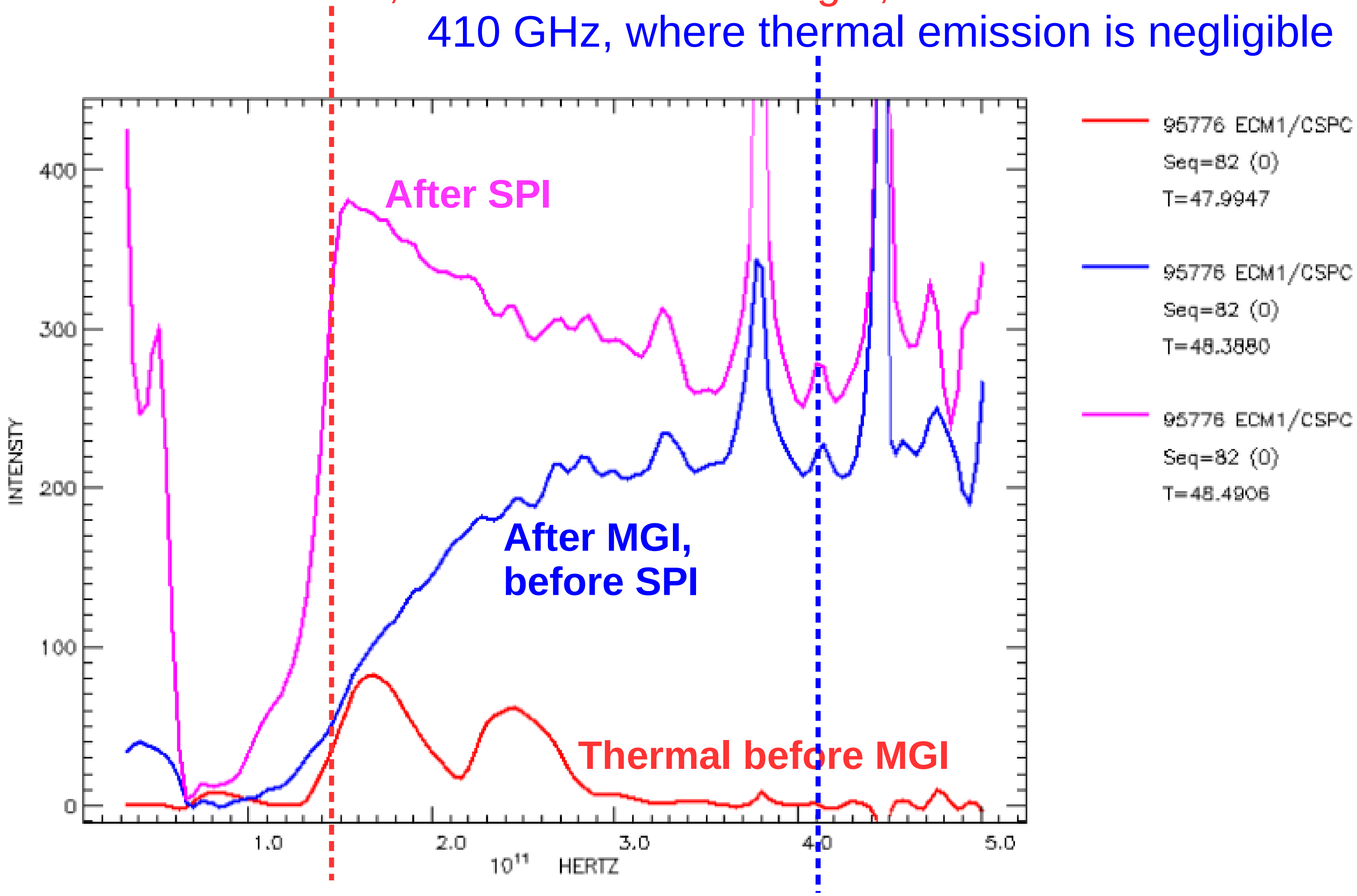

ECE evolution at 146 and 410 GHz

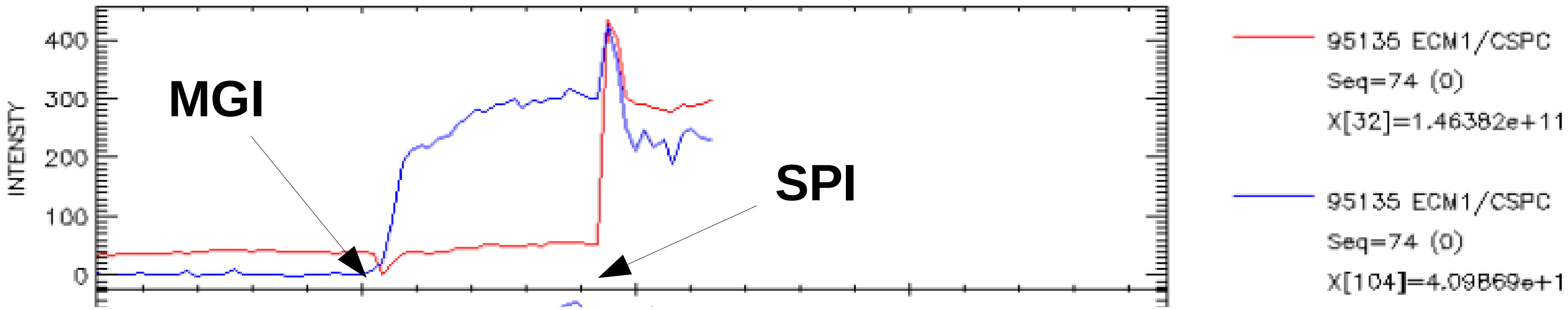

- Prompt response to MGI of the high-frequency component
- The low-frequency component jumps and overrides after SPI.

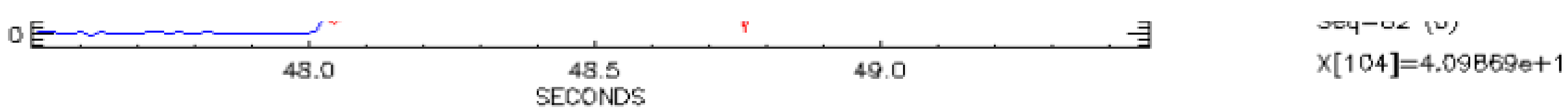

ECE evolution at 146 and 410 GHz

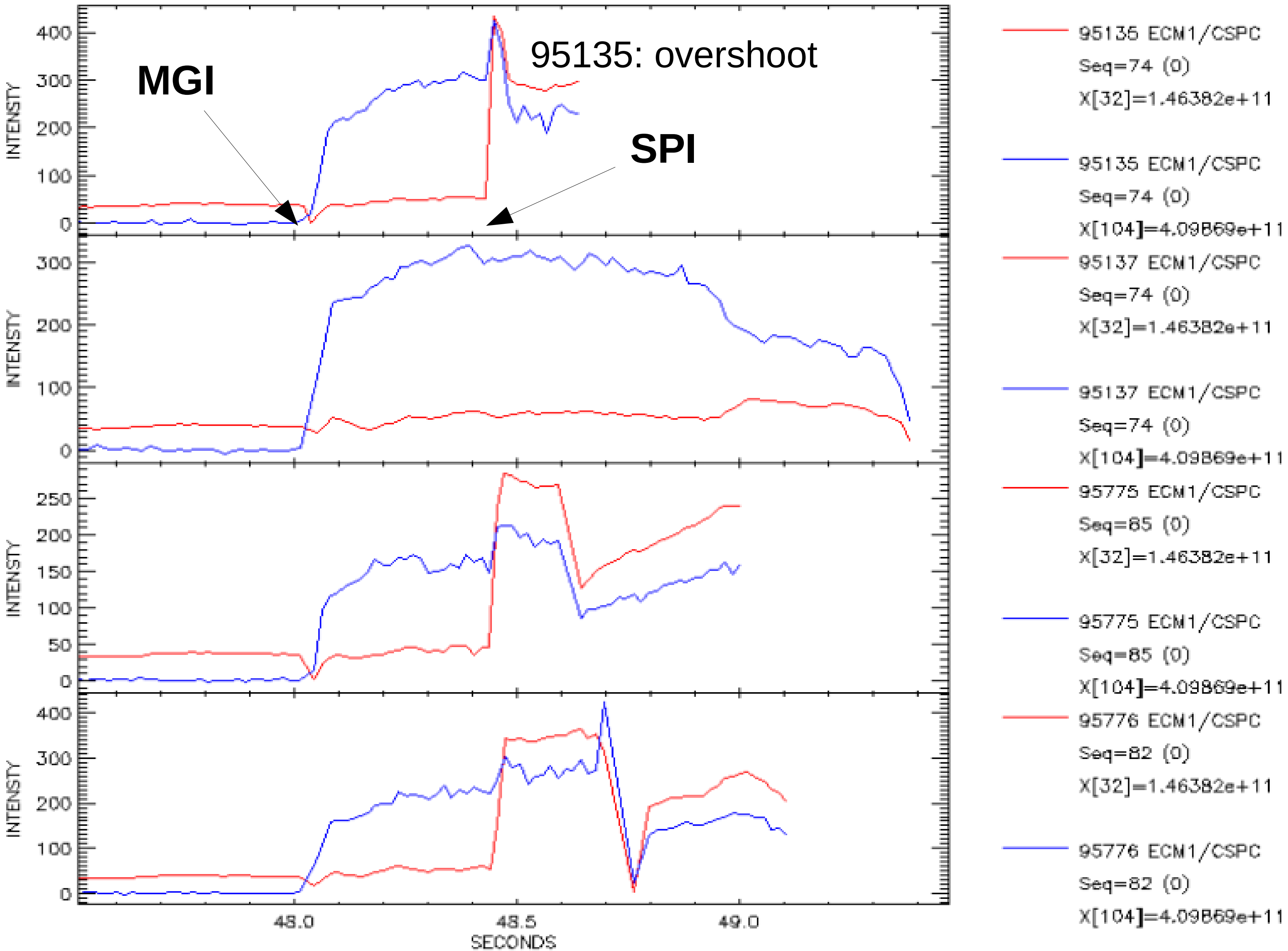

ECE evolution at 146 and 410 GHz

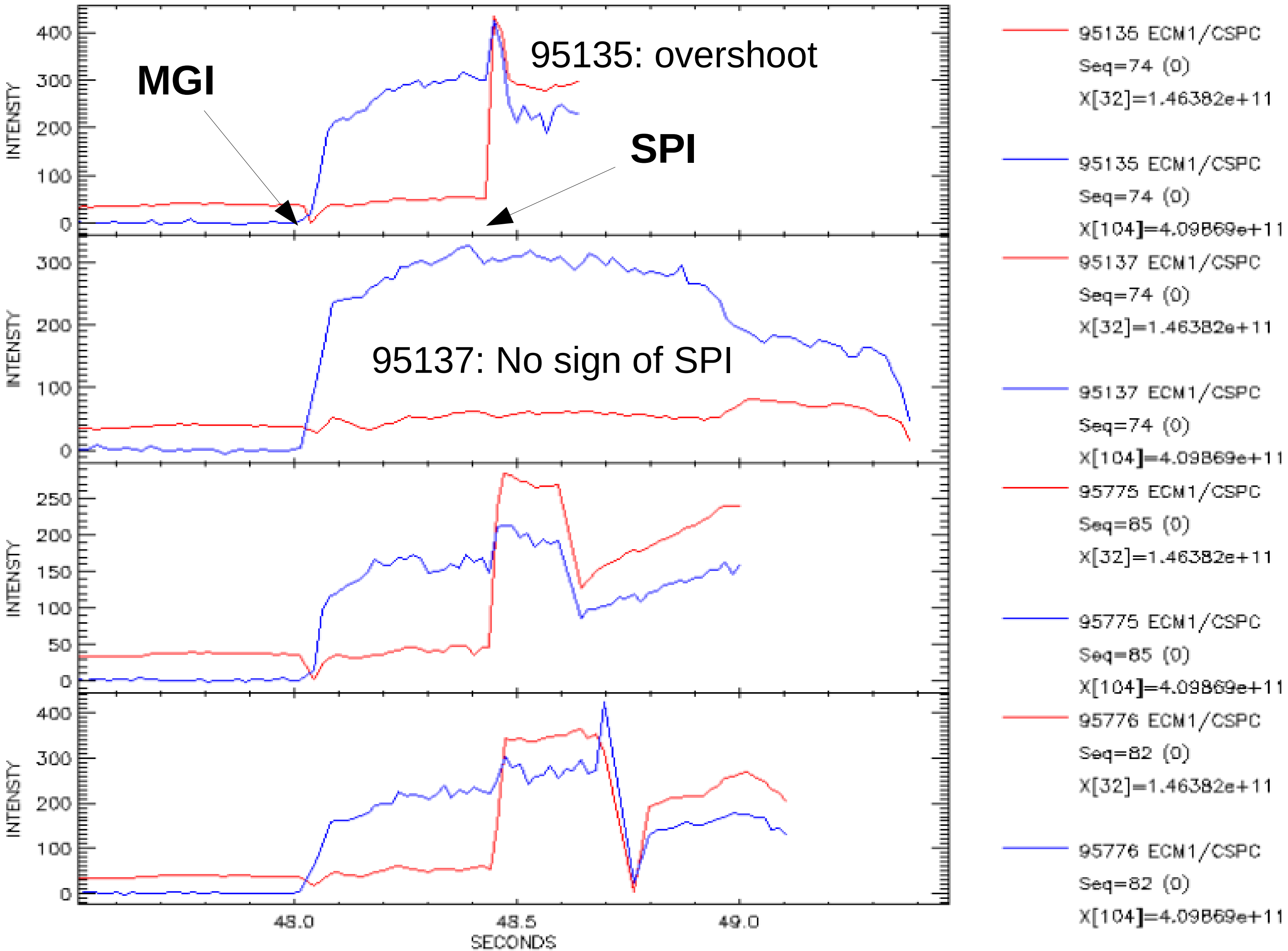

ECE evolution at 146 and 410 GHz

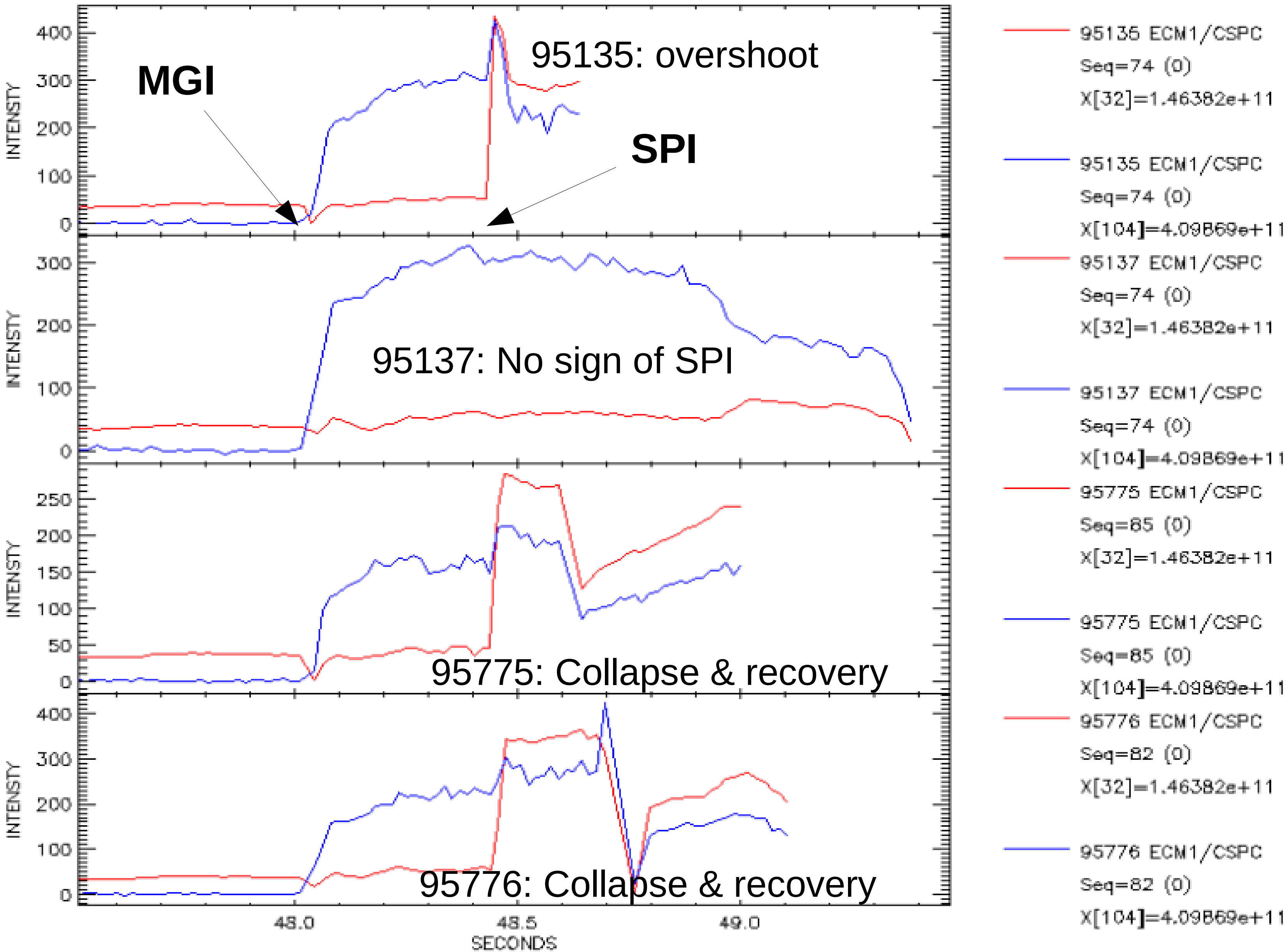

ECE spectra after collapse

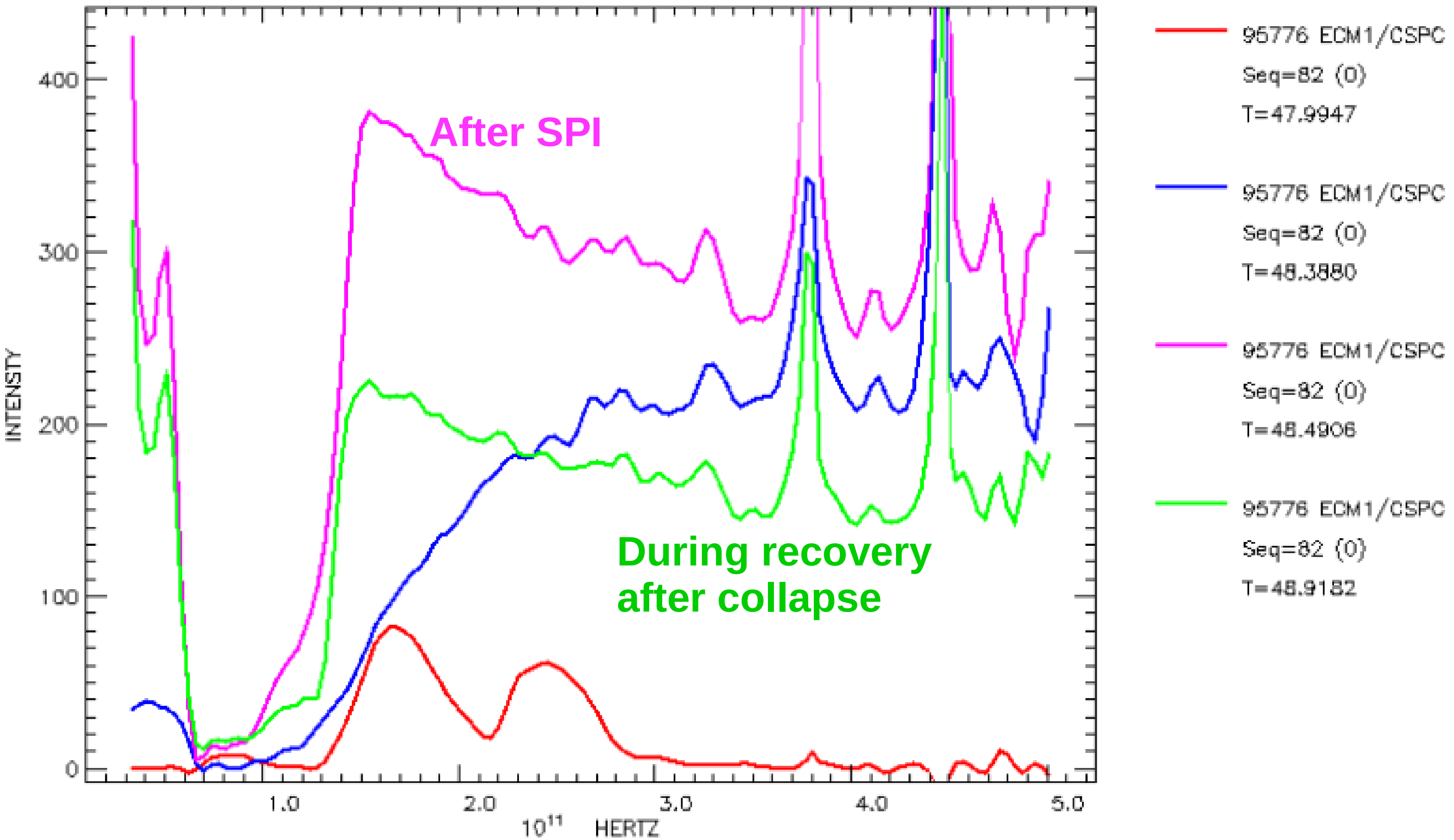

Spectral shape during recovery after collapse remains similar to the post-SPI one.

ECE - IR camera comparison

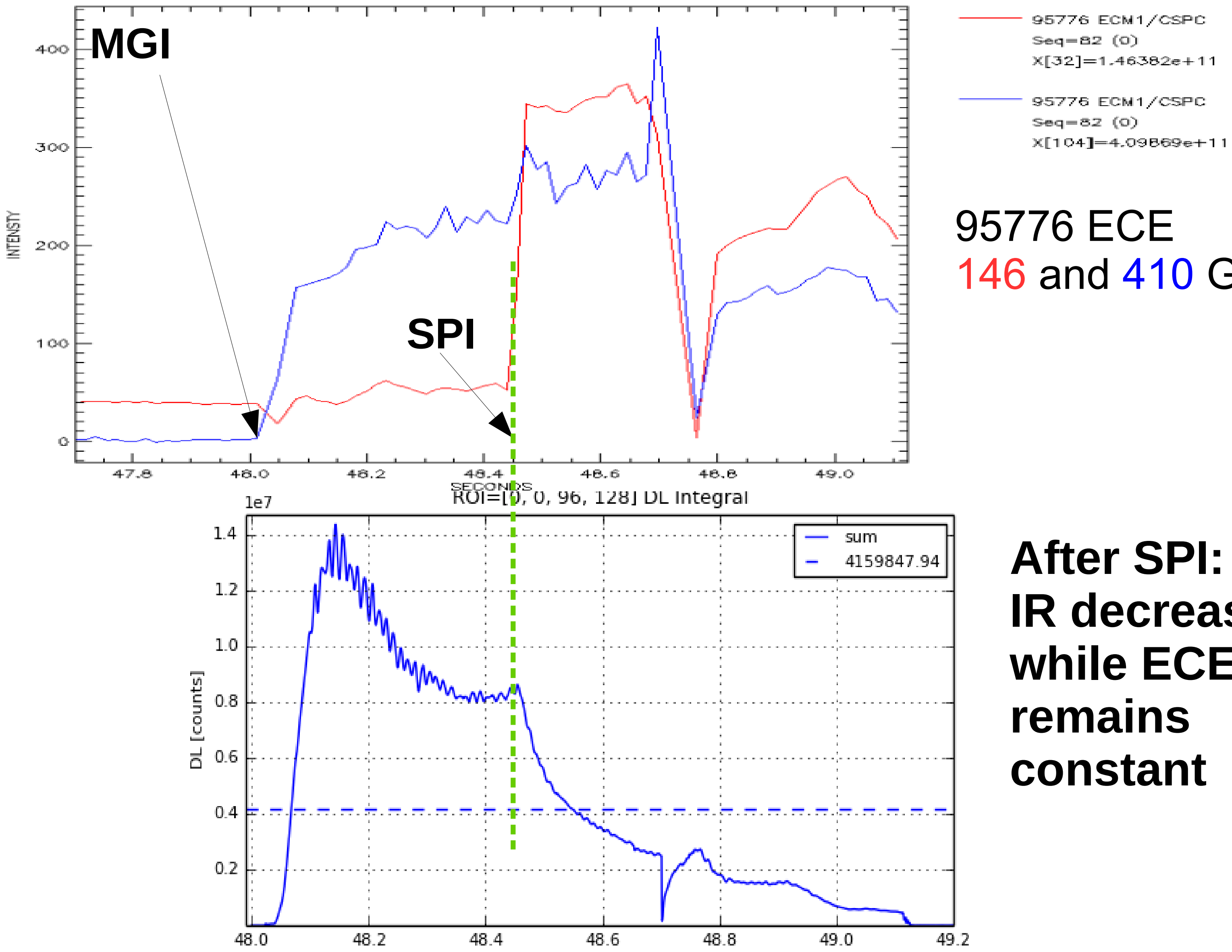

95776 ECE
146 and 410 GHz

After SPI:
IR decreases while ECE remains constant

Synchrotron emission toy model

- Synchrotron emission is a strong function of wave field variation across the Larmor orbit:

$$k_{\perp}\rho_L = \frac{\omega}{\omega_{ce}} N \sin\theta \, p_{\perp}$$

- Where the refractive index $N = kc/\omega$ and $\theta = \angle(\mathbf{B}, \mathbf{k})$

- Emission increases throughout the spectrum for increasing $p_{\perp}$

- Emission decreases if $N(\omega, \theta, B, n_e)$ decreases

Refractive index

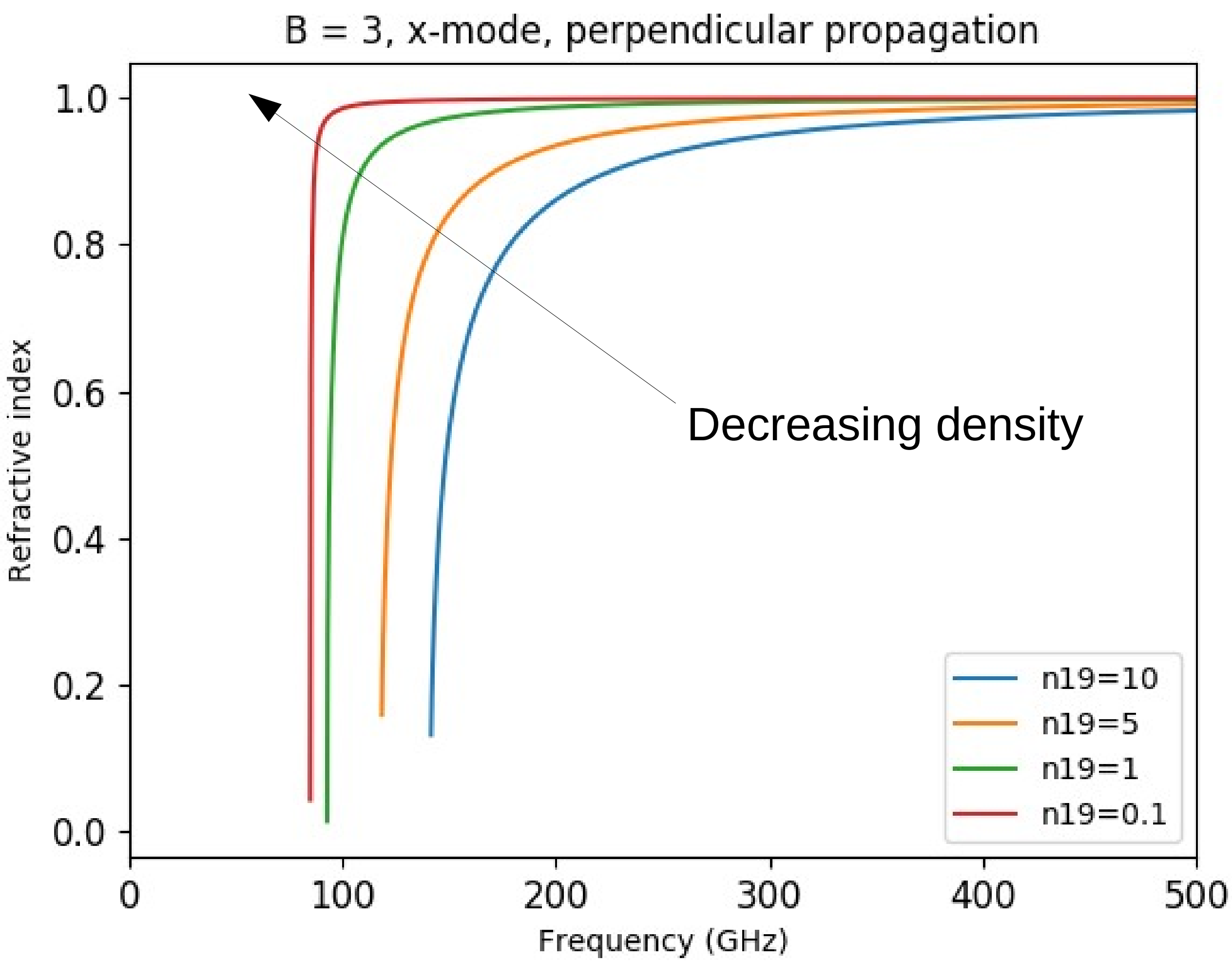

- As density decreases, the refractive index increases and the cutoff shifts to the left

The toy model

- Not-too-dense beam in a cold background plasma: **optically thin emission**
- Sum emission by individual RE **dressed** by the background plasma density
- The emitting region length is enhanced by multiple wall reflections
- Uniform, dispersive but not absorbing background plasma
- Uniform magnetic field
- Assume a population of identical RE

Wall reflections

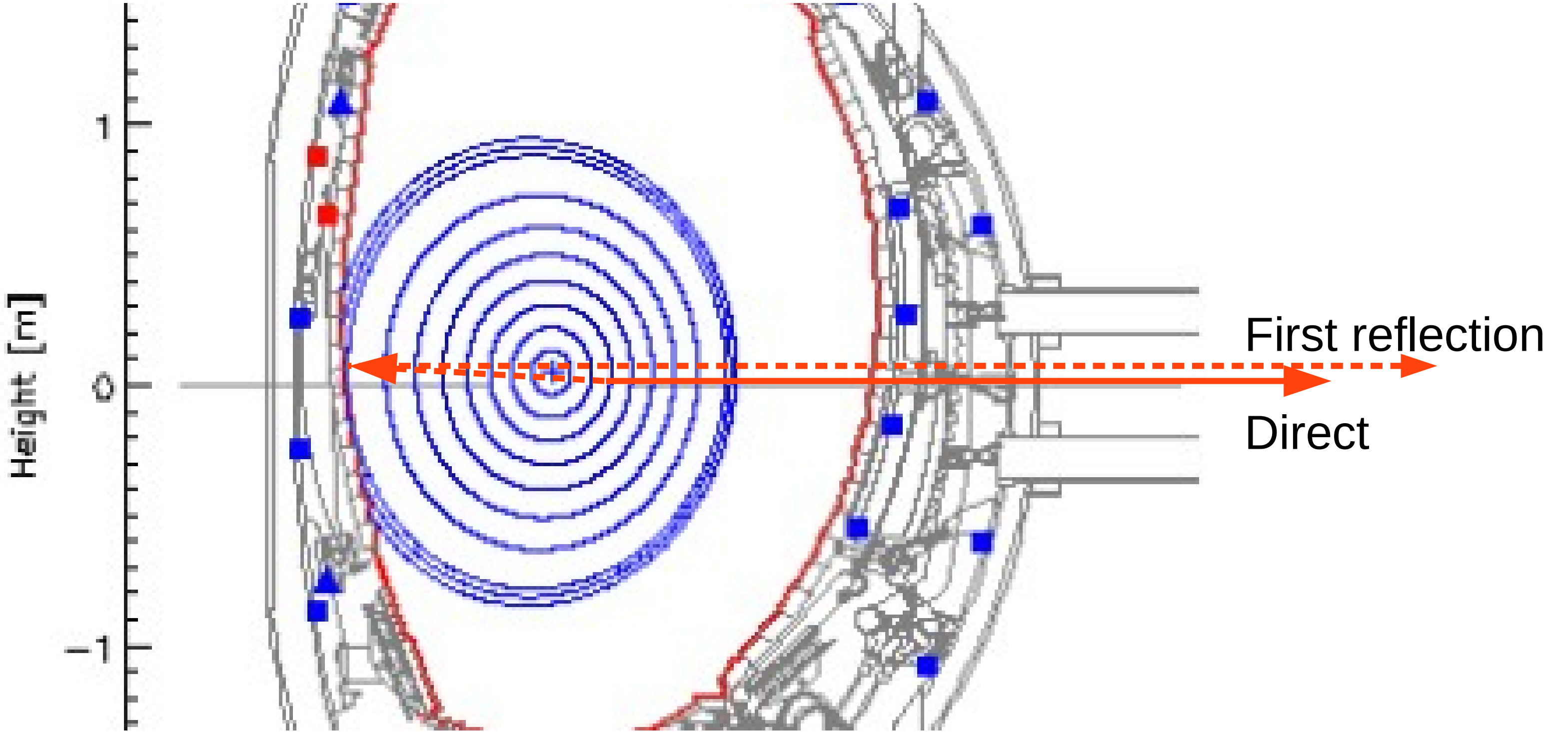

- If the plasma is optically thin, emission is enhanced by multiple wall reflections
- The effect is equivalent to increasing the length of the emitting region
- The enhancement could be estimated from analysis of thermal emission at the third harmonic

The toy model

- Power from an electron per unit frequency and solid angle:

$$\frac{\mathrm{d}P_\pm}{\mathrm{d}\omega\,\mathrm{d}\Omega} = \eta_\pm(\omega, \theta, \mathbf{p}, \omega_{ce}, \omega_{pe})$$

where $\pm$ indicates polarization mode

- ECE measures intensity averaged over the angular response $w(\theta)$
- For a population of identical electrons

$$I_\pm = n_{RE}\, l \int w(\theta)\, \eta_\pm \mathrm{d}\Omega$$

where *l* is an effective path length given by the beam diameter divided by *w(0)*.

Dressed emission

$$I_{\pm} = n_{RE} l \, \frac{e^2 \omega}{4\pi\epsilon_0 c \beta_z} \sum_n w(\theta_n) \, N_{\pm} \frac{\partial(\omega N_{\pm})}{\partial \omega} \frac{2\omega}{E_i E_j^* \frac{\partial}{\partial \omega}(\omega^2 \epsilon_{ji})} |E_i \, \Gamma_i^{n*}|^2$$

Refractive index

Polarization vector

Dielectric tensor

$$E_i \, \Gamma_i^{n*} = E_x \, \frac{n\omega_{ce}}{\gamma \omega N_{\pm} \sin\theta} \mathrm{J}_n(k_\perp \rho_L) - iE_y \, \beta_\perp \mathrm{J}_n'(k_\perp \rho_L) + E_z \, \beta_z \, \mathrm{J}_n(k_\perp \rho_L)$$

Al quantities calculated at θ_n given by

$$N_{\pm}(\theta_n) \cos\theta_n = \frac{1}{\beta_z} \left(1 - \frac{n \, \omega_{ce}}{\gamma \, \omega} \right)$$

ECE angular response and units

- Lorentzian model for the angular response $L(x) = \frac{1}{1+x^2}$

$$w(\theta) = \frac{L((\theta - \pi/2)\,/\,\delta)}{\int L((\theta - \pi/2)\,/\,\delta)\,\mathrm{d}\Omega}$$

- Sum polarizations assuming that wall reflections scramble them
- and use ECM1 units: pW instead of W and Hz instead of rad/s

$$I_{ECM1} = \frac{10^{12}}{2\pi}(I_+ + I_-)$$

- The toy model is available as a Jupyter (.ipynb) notebook

ECE spectra

- Population of identical RE with p=8 and large (0.9) pitch angle

$$\frac{I_{ECM1}}{n_{RE}\, l}$$

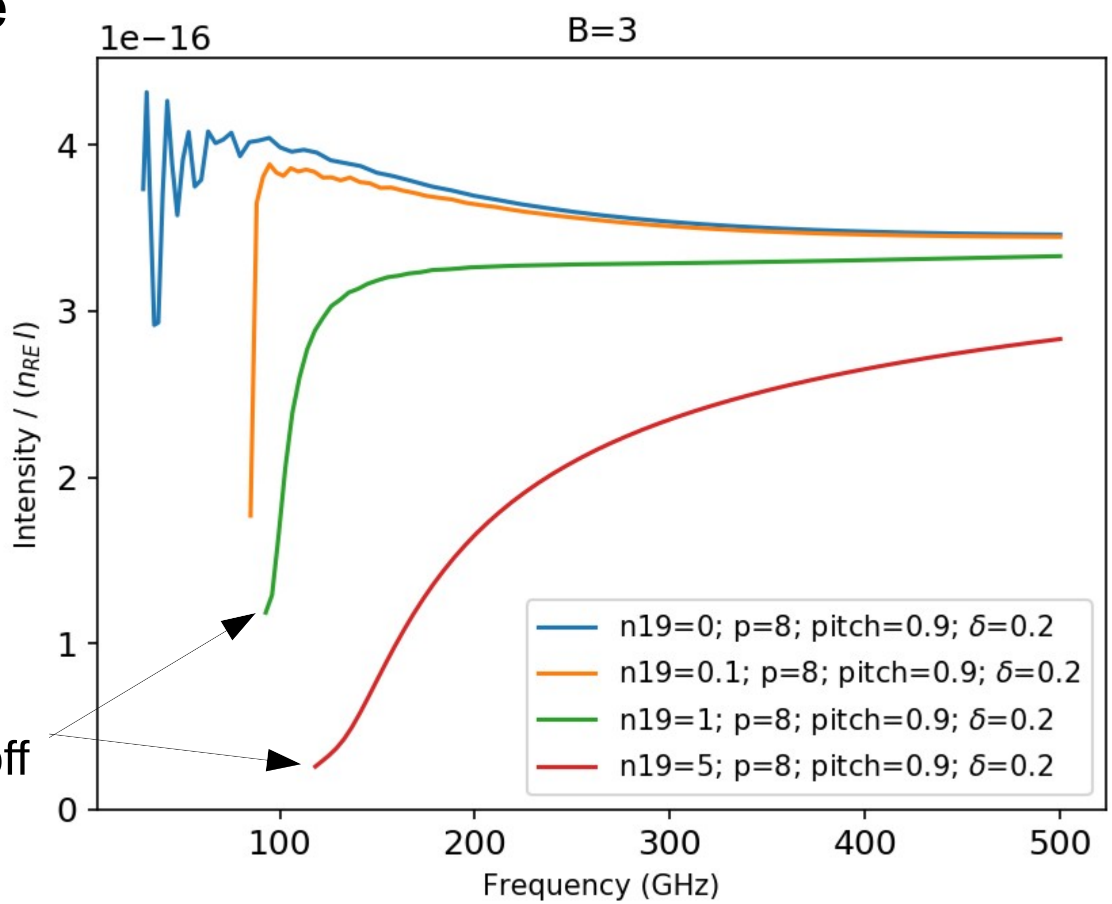

Spectra start at the x-mode cutoff

- Density scan: spectral shape changes dramatically
- From “MGI” to “SPI” shape as density decreases.

ECE spectrum calculation

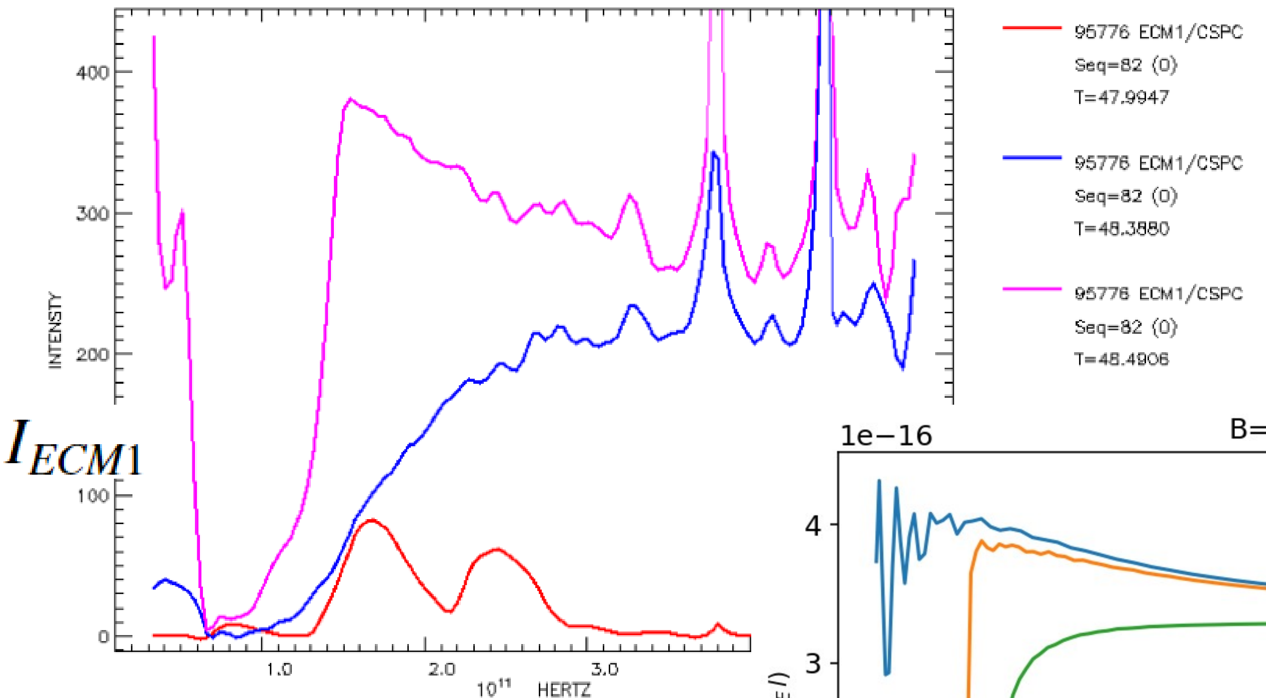

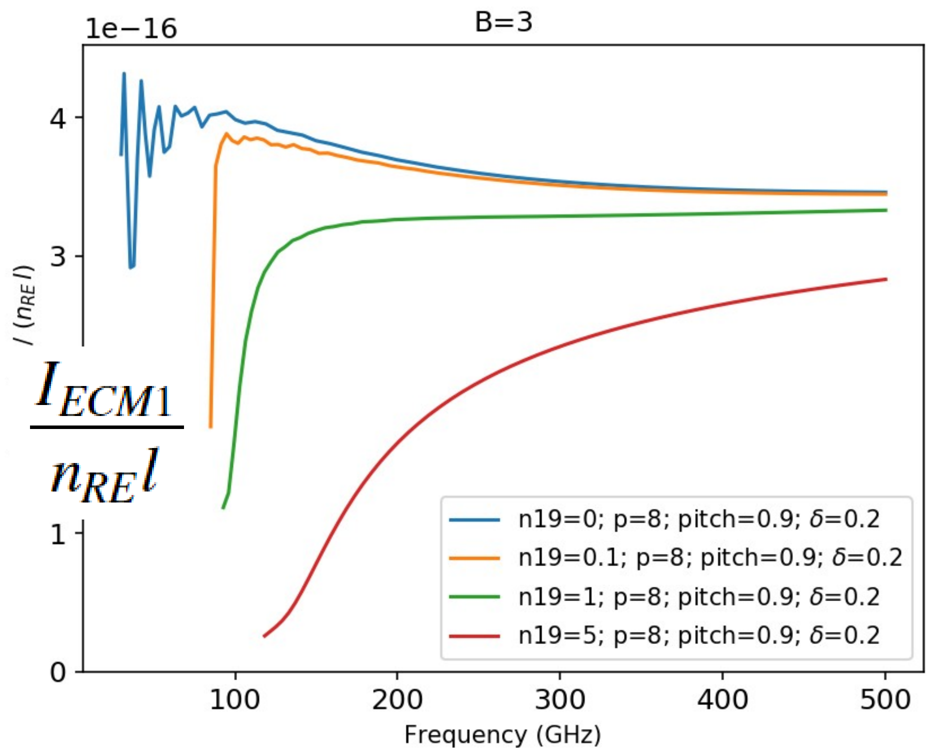

- $n_{RE} l \approx 10^{18}\ \mathrm{m}^{-2}$
- with $l \approx 10\ \mathrm{m}$:

  $n_{RE} \approx 10^{17}\ \mathrm{m}^{-3}$

ECE from low-energy electrons

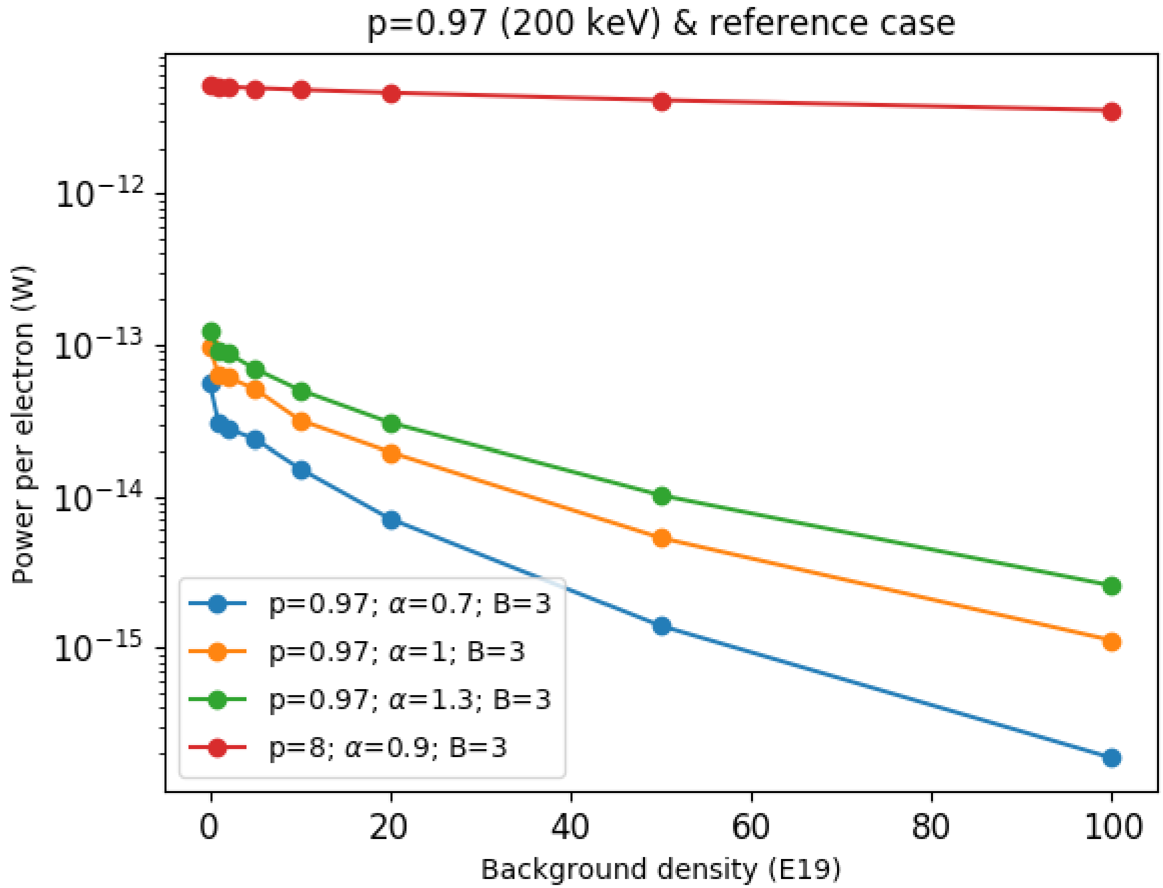

- Power per electron in the reference case (prev. slide) changes from 5.5 to 3.5E-12 for a density variation from 0 to E21
- The relative variation is much larger at lower electron energy (shown 200 keV case) but ...

ECE from low-energy electrons

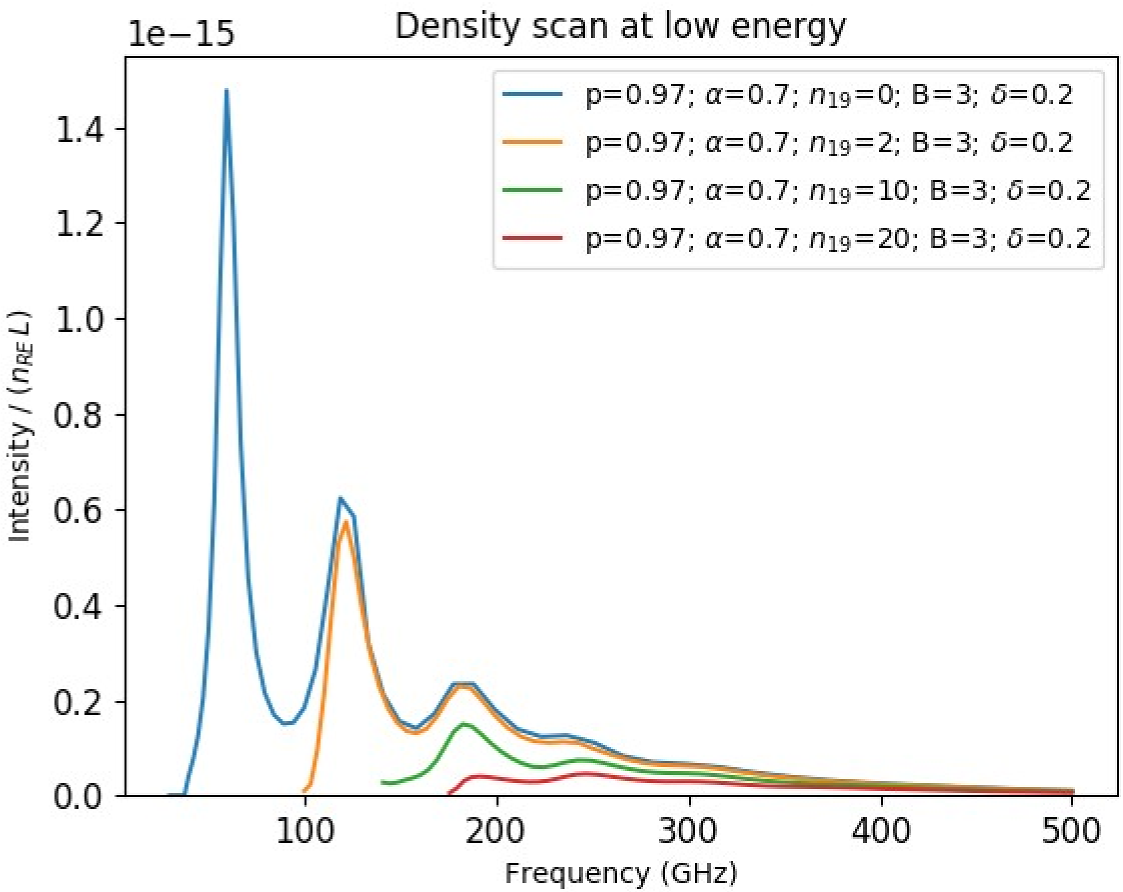

- … but calculated ECE spectra for 200 keV do not resemble measured ones, in particular intensity strongly decreases with frequency above 300 GHz.

ECE from high-energy electrons

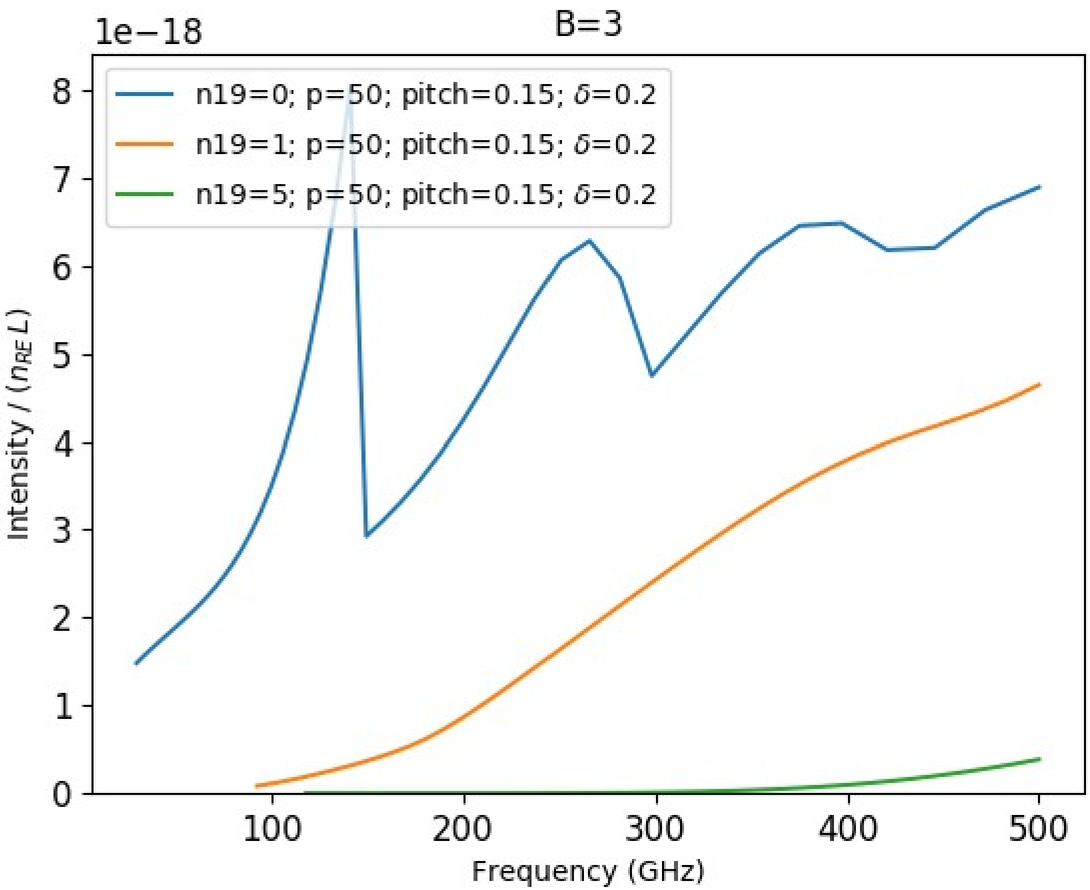

- Electron parameters typical of synchrotron emission in the VIS: 25 MeV, pitch angle = 0.15
- With this, emission is reduced by two orders of magnitude, due to forward radiation beaming

ECE - IR camera comparison

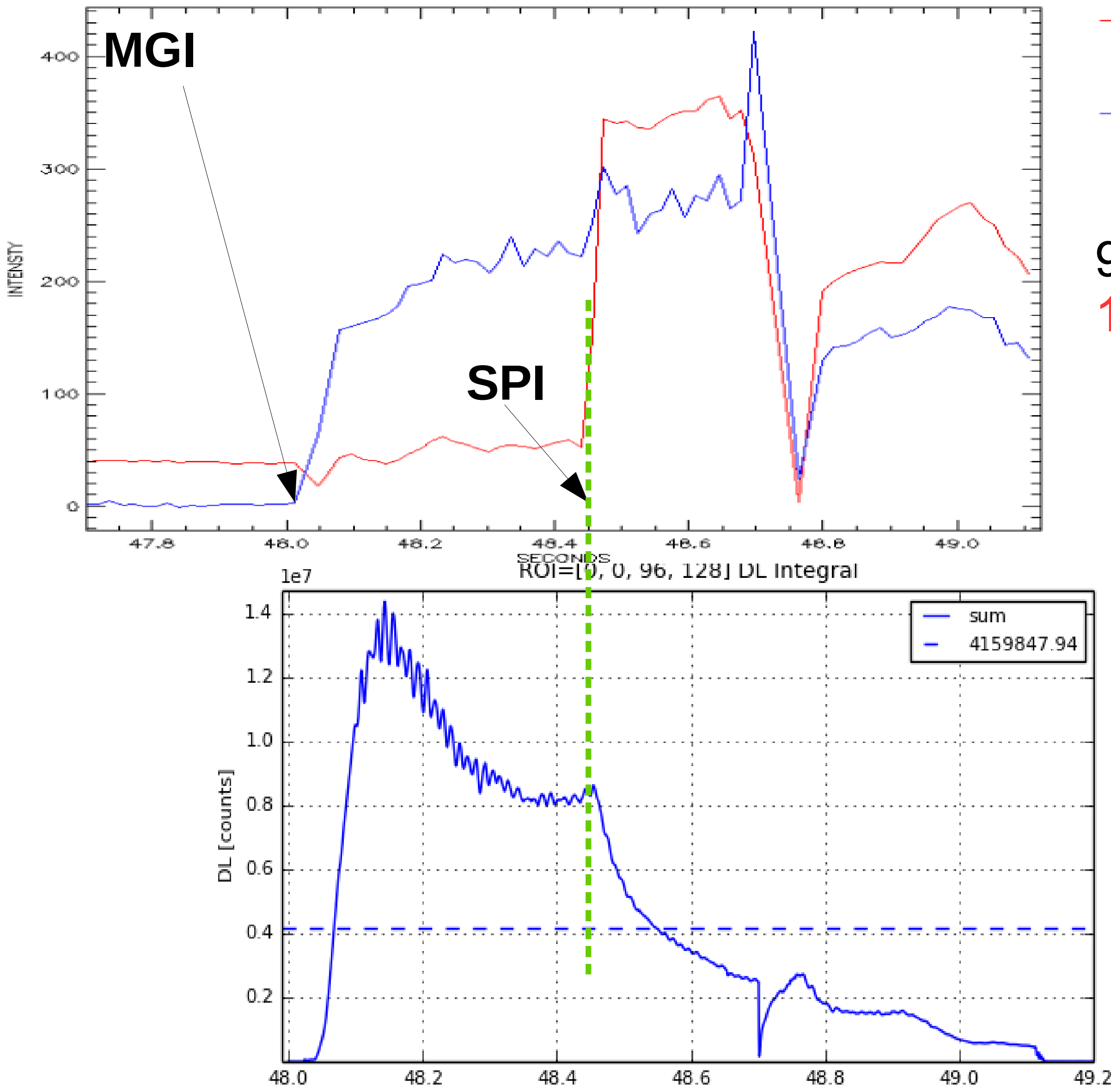

95776 ECE
146 and 410 GHz

After SPI:
IR decreases while ECE remains constant

IR from higher energy RE

Fast ECE evolution

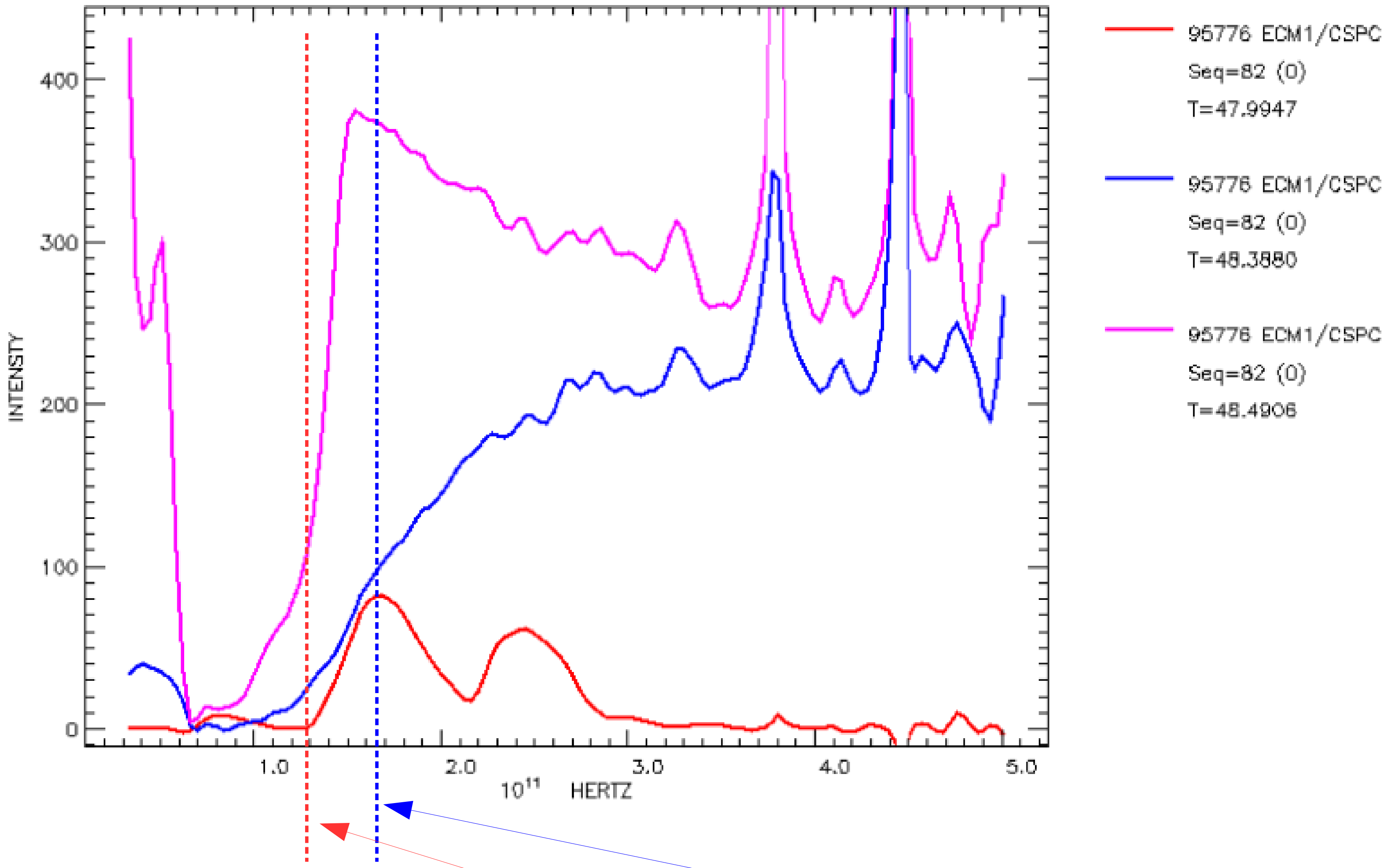

Next: fast response to SPI at 127.8 and 163.6 GHz from KK3F

ECE response time from KK3F

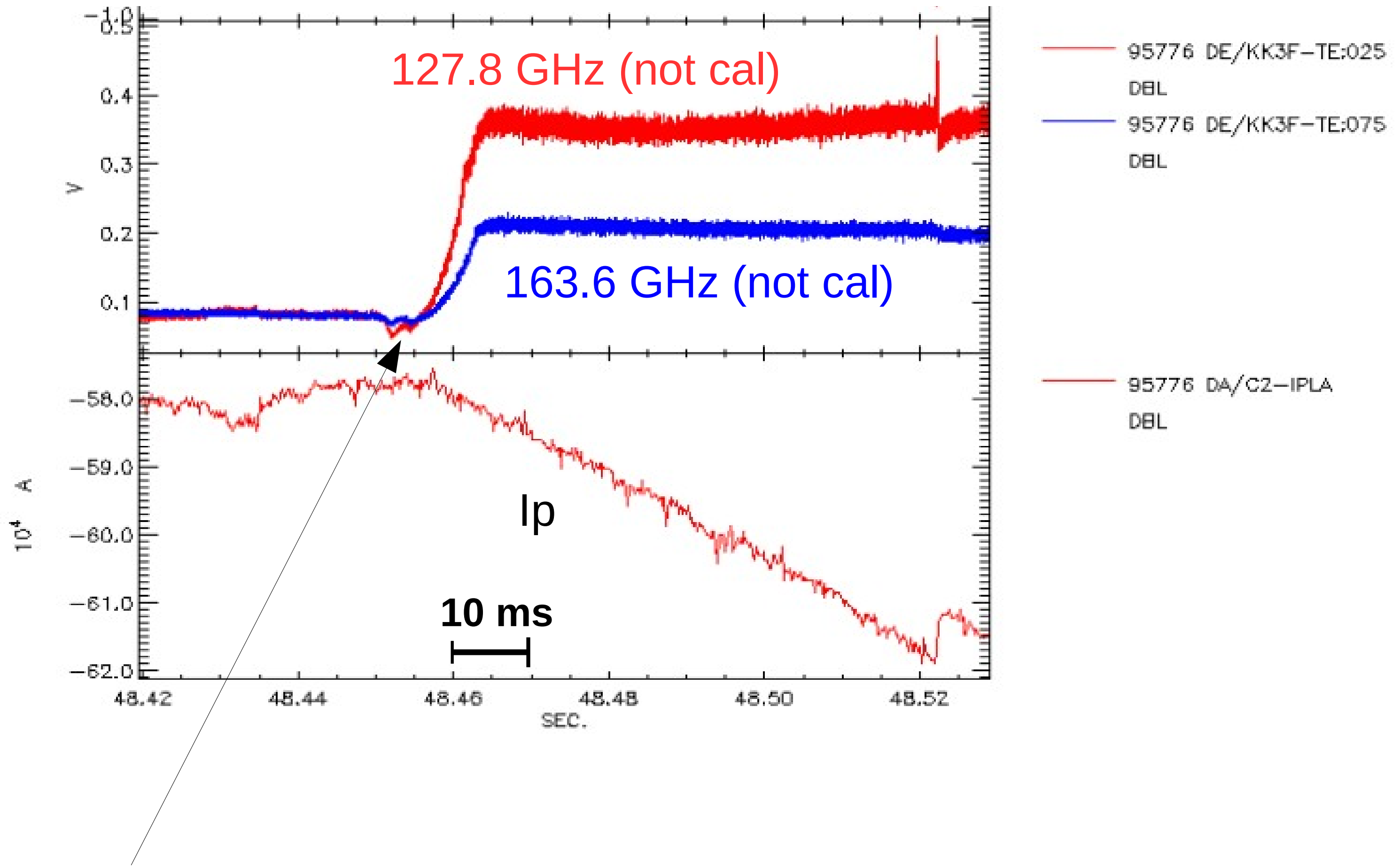

- 5-10 ms duration of ECE increase after SPI

ECE and MHD spikes

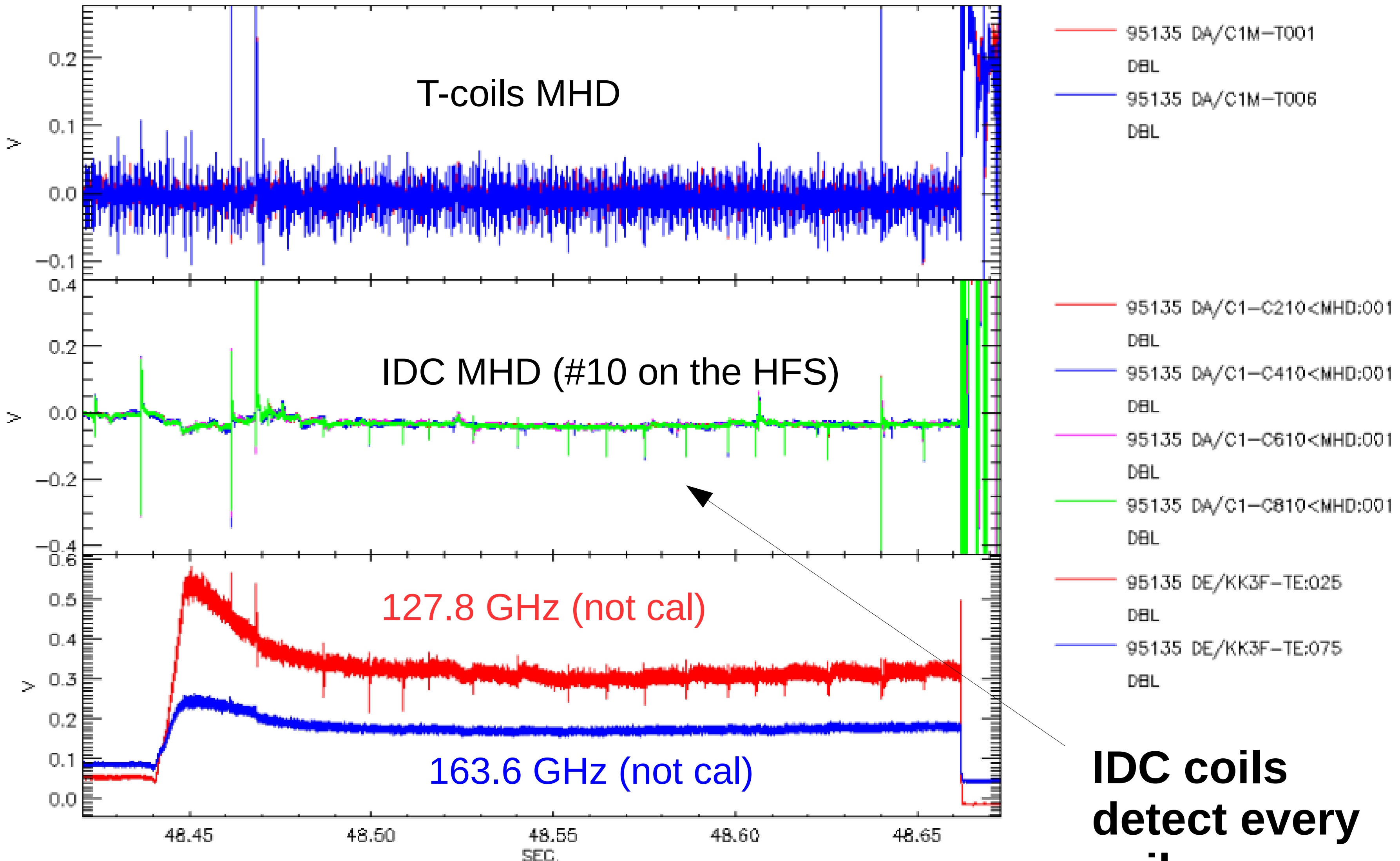

IDC coils detect every spike

ECE and MHD spikes

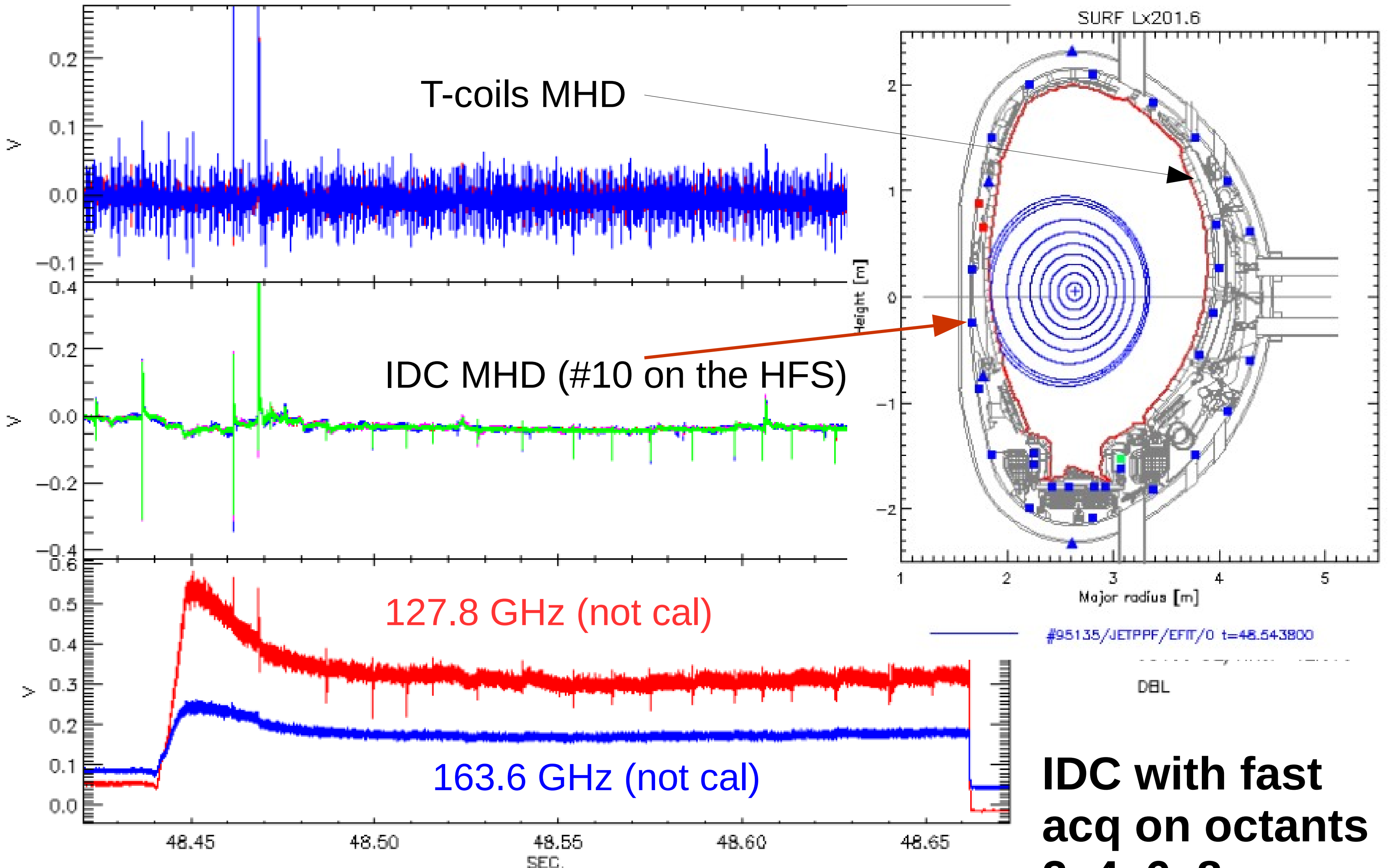

IDC with fast acq on octants 2, 4, 6, 8

Fast ECE evolution

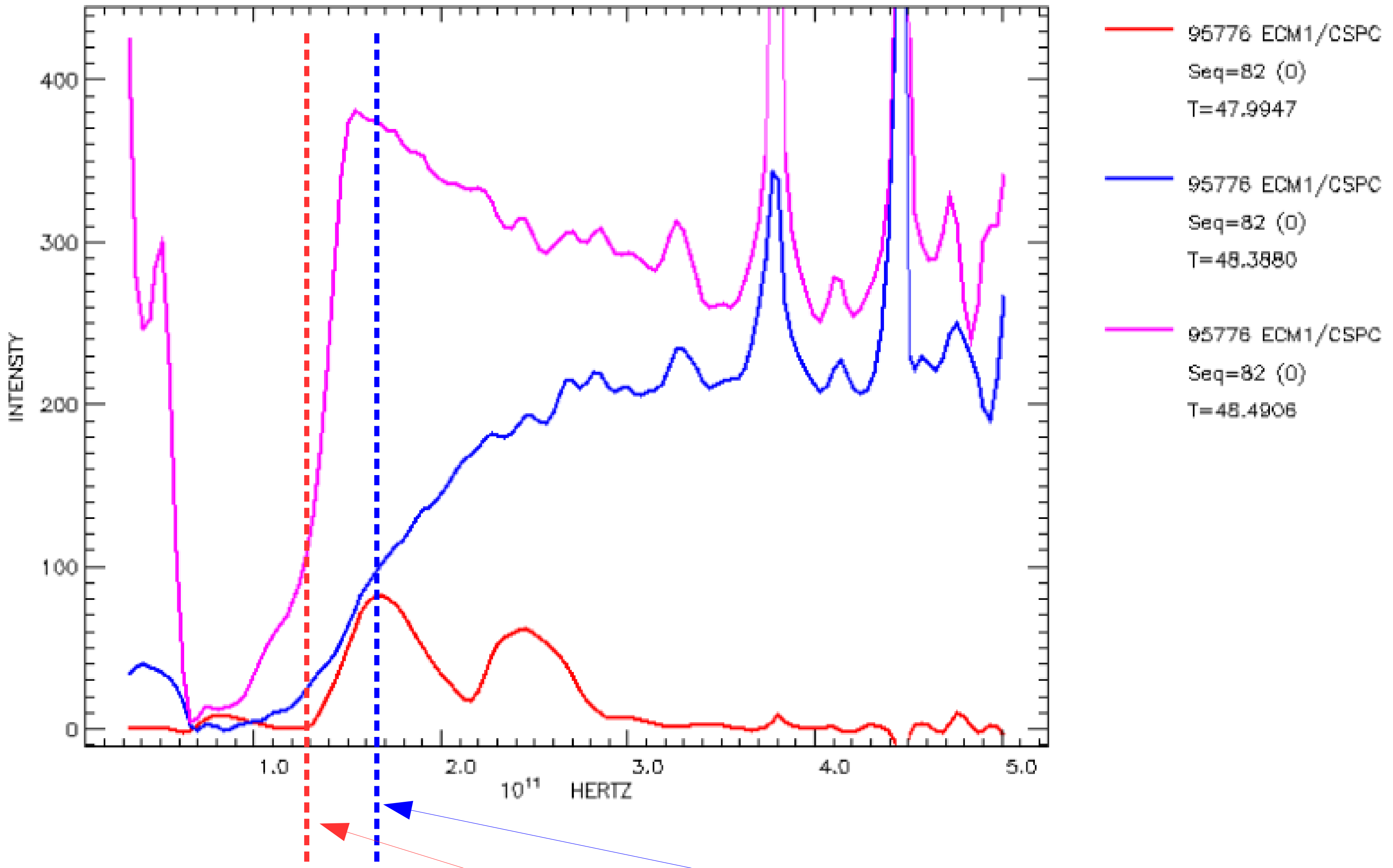

Next: fast response to SPI at 127.8 and 163.6 GHz from KK3F

ECE and MHD spikes

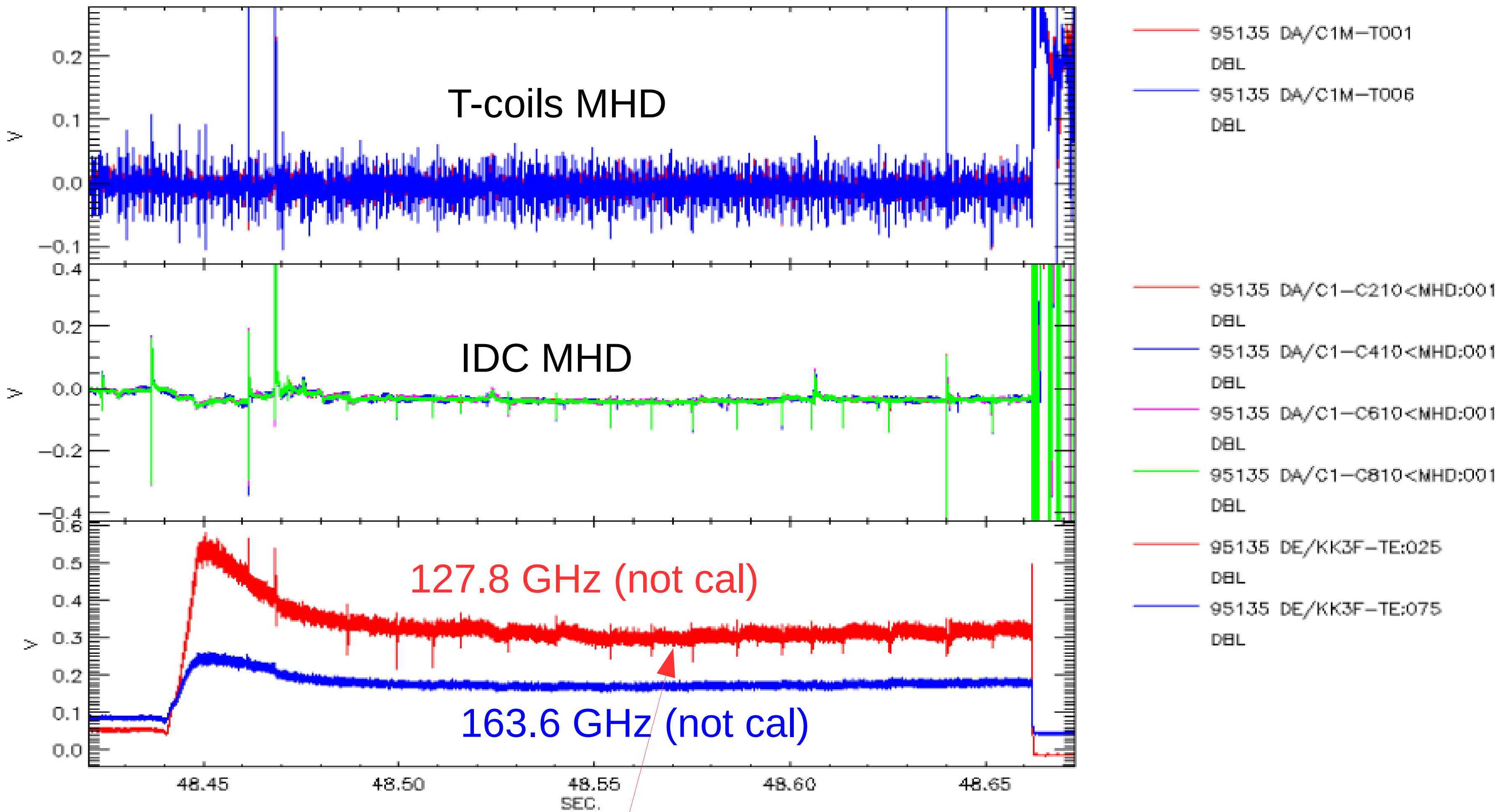

- ECE spikes are only visible in channels close to the x-mode cutoff, like the one at 127.8 GHz.
- Most likely this is an effect of changes of the background density, and not of the RE distribution.

Summary

- ECE at low frequencies dramatically increases with SPI.
  - ECE increase is compatible with a strong reduction of the background plasma density
  - The change takes place in 5-10 ms

- Fast transients are captured by ECE and HFS coils
  - Transients appear as cutoff variations (due to gas release caused by MHD instabilities) and not as pitch-angle-scattering events.

ECE vs popular synchrotron formula

$$\frac{dP_e}{d\lambda} = \frac{c\, e^2}{\sqrt{3}\, \epsilon_0\, \gamma^2\, \lambda^3} \int_{\lambda_c/\lambda}^{\infty} K_{5/3}(z)\, dz \qquad \lambda_c = \frac{4\pi}{3}\, \frac{R}{\gamma^3}$$

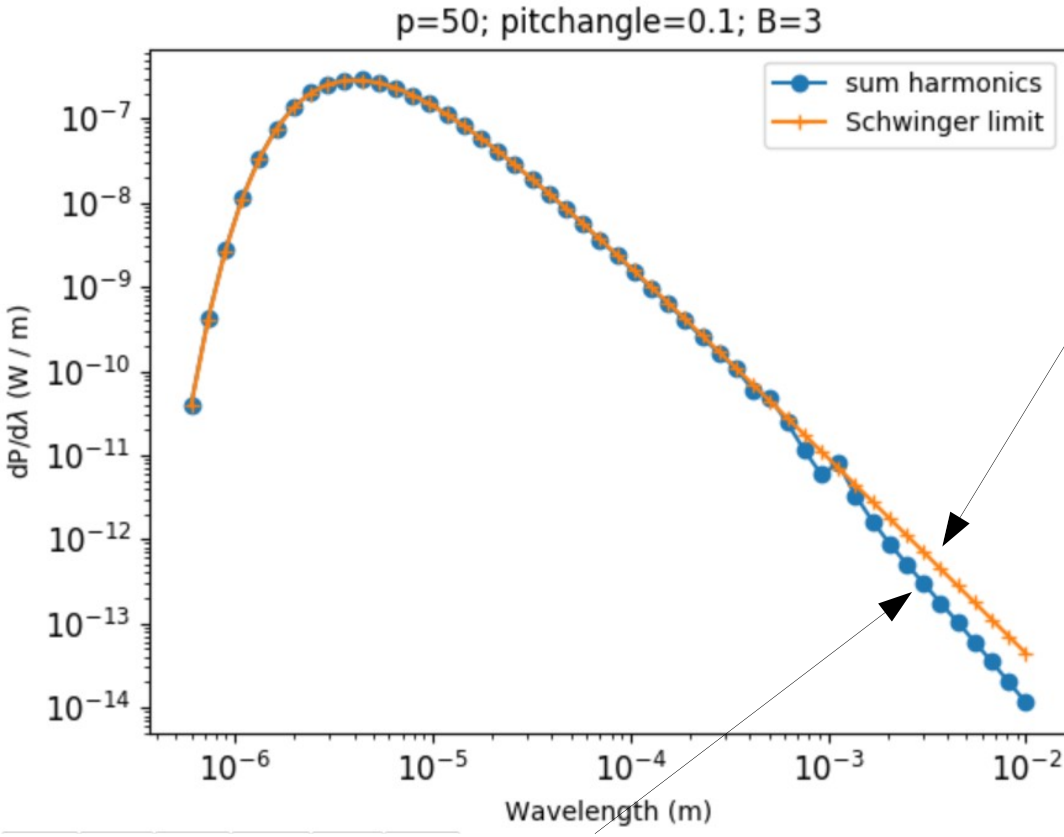

Agreement in IR and visible range (used as a benchmark)

Deviations in the 30-500 GHz range, where the Schwinger approximation fails because individual harmonics do matter.

$$\frac{dP}{d\lambda} = \frac{2\pi\, c}{\lambda^2}\, \frac{dP}{d\omega} = \frac{2\pi\, c}{\lambda^2} \sum_{\pm} \int \eta_{\pm}\, d\Omega$$